Review of non-linear Compton scattering experiments and prospect for Unruh radiation experiment

T. Tauchi, KEK

an informal workshop on physics in high intensity fields,
Hayama campus of Sokendai, 9-10 December, 2012

Present/previous and future Lasers

	laser power (mJ)	laser freq. (Hz)	laser pulse length (fs)	laser pulse length (um)	power (TW)	laser spot size σ (um)	Laser spot area $A_{eff}(um^2)$	laser density (W/cm^2)	laser wave length (nm)	(eV)	E_{rms} (V/cm)	a_o or η	refrection index
	f		$t=\sqrt{(2\pi)}\,\sigma_t$		f/t	rl (σ_x)	$2\pi\,\sigma_x\sigma_y$	$f/2\pi\,\sigma_x\sigma_y t$	λ	$h\nu$	$\sqrt{\{Z_o I\}}$, $Z_o=377\Omega$	$eE_{rms}/\omega mc$	$\Delta n=14\,\alpha\,E^2/(45\pi\,E^2_{crit})$
SLAC-FFTB IR	800	0.5	1,504	451	0.53	3.01	56.9	9.36.E+17	1,053	1.18	1.88.E+10	0.61	1.46.E-15
SLAC-FFTB Green	500	0.5	1,504	451	0.33	2.2	30.7	1.08.E+18	527	2.35	2.02.E+10	0.33	1.69.E-15
BNL	4,000		30,000	9000	0.13	27	4578.1	2.91.E+15	10,600	0.12	1.05.E+09	0.35	4.56.E-18
ATF2-IPBSM(Shintake M.)	1,500	10	8,000,000	2,400,000	0.00019	15	1413.0	1.33.E+13	532	2.33	7.07.E+07	0.0012	2.08.E-20
ATF2-200TW-a60	6,000	10	25	7.5	240	0.50	1.6	1.52.E+22	800	1.55	2.39.E+12	59.53	2.38.E-11
ATF2-200TW-a10	6,000	10	25	7.5	240	3.01	56.9	4.22.E+20	800	1.55	3.99.E+11	9.92	6.61.E-13
ATF2-20TW-a2	600	10	25	7.5	24	4.51	127.9	1.88.E+19	800	1.55	8.41.E+10	2.09	2.94.E-14
J-KAREN	5,000	0.00056	40	12	125	3.75	88.3	1.42.E+20	800	1.55	2.31.E+11	5.75	2.21.E-13
Schwinger field								4.65.E+29		1.55	1.32.E+16	3.3.E+05	7.28.E-04
ELI-goal	3,000,000	0.017	30	9	100,000	5	157.0	1.00.E+26		1.55	1.94.E+14	4.8.E+03	1.56.E-07
PFS@MPI	5,000	10	5	1.5	1,000	3.01	56.9	3.00.E+23	1,035	1.20	1.06.E+13	342.21	4.69.E-10
HERCULES, Michigan	9,000	0.1	30	9	300	0.5	1.6	1.91.E+22	800	1.55	2.68.E+12	66.76	2.99.E-11
Astra Gemini@RAL.uk	15,000	0.05	30	9	500	0.9	5.1	9.83.E+21	800	1.55	1.93.E+12	47.88	1.54.E-11
POLARIS@Jena.de	150,000	0.1	150	45	1,000	3.01	56.9	1.76.E+21	1,035	1.20	8.14.E+11	26.20	2.75.E-12
Osaka-ILE-LFEX	10,000,000	3.472E-05	1,000	300	10,000	10	628.0	1.59.E+21	1,050	1.18	7.75.E+11	25.29	2.49.E-12
AIST@Tsukuba	135	10	135	41	1	12	904.3	1.11.E+17	800	1.55	6.46.E+09	0.16	1.73.E-16
BNL - stage-2	30,000		30,000	9000	1.00	27	4578.1	2.18.E+16	10,600	0.12	2.87.E+09	0.95	3.42.E-17

Intense Laser and Electron・Photon Interaction

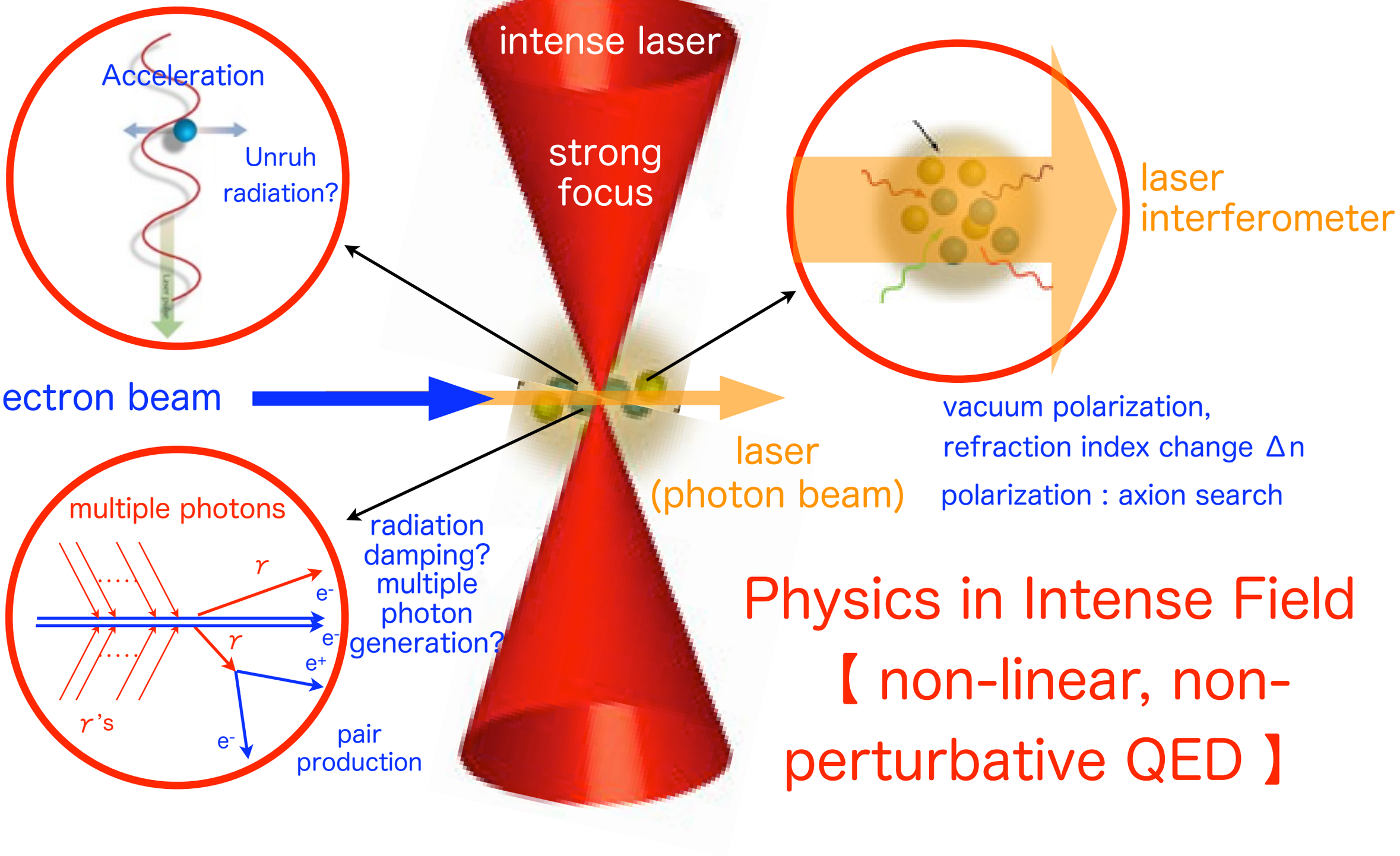

Physics in Intense Field 【 non-linear, non-perturbative QED 】

BNL experiment, PRL 96, 054892(1996)

deposit/shot in Si diode
1.1×10^{11} eV (2×10^{7} photons)
2.6×10^{9} eV w/ A_g foil
1.3×10^{9} eV bremsstrahlung

a_0=0.35, λ=10.6μm
4J in 30psec (FWHM)
27μm(rms)

2nd stage :
a_0=0.95, λ=10.6μm
30J in 30psec (FWHM)
27μm(rms)

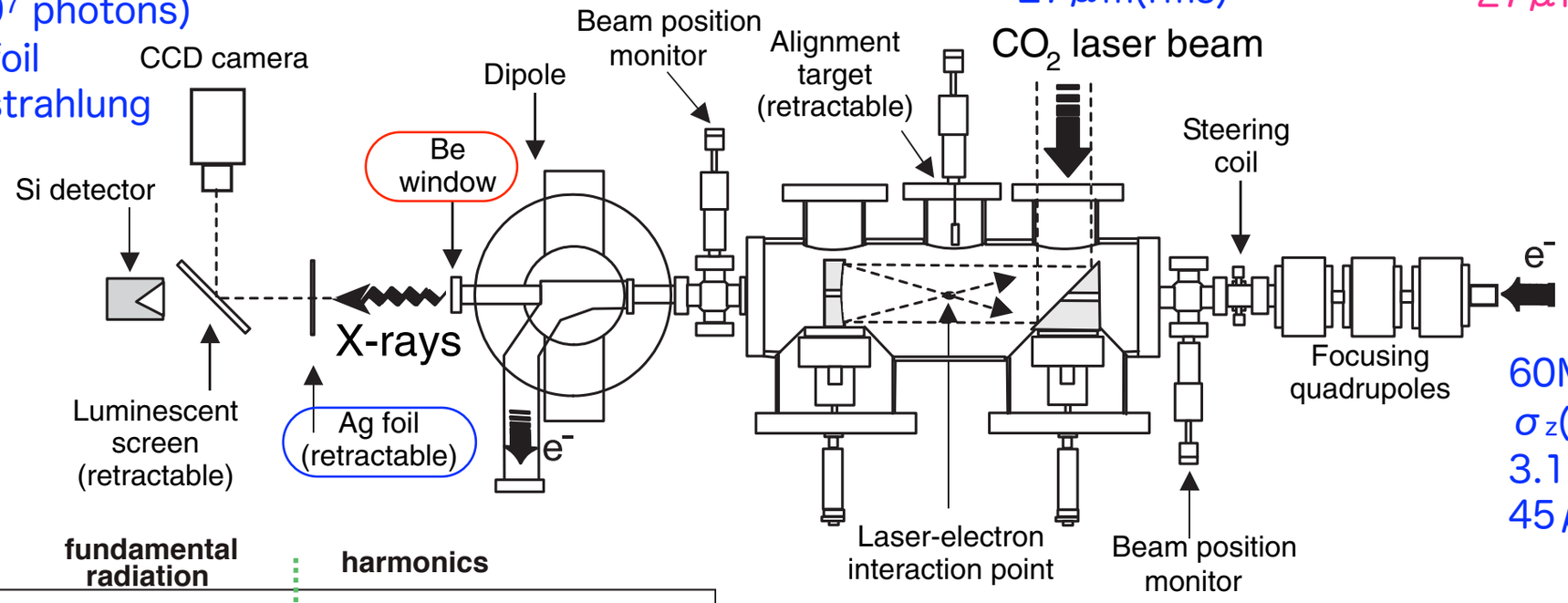

60MeV
σ_z(FWHM)=1.1 mm
3.1×10^{9}(0.5nC)/bunch
45μm x 80μm(rms)

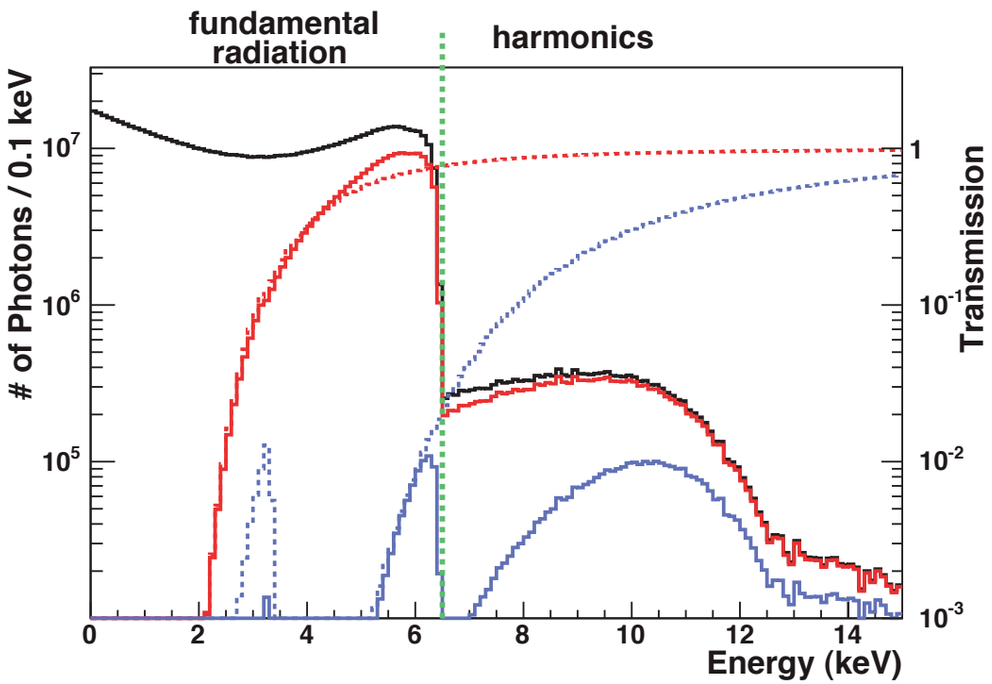

FIG. 2 (color). Simulated energy spectra of Thomson x rays. Solid lines: (black line) at the interaction point; (red line) on the detector after attenuation in the Be window and air; (blue line) filtered by a 10 μm Ag foil. Dashed lines show combined spectral transmission of the Be window with air (red line) and Ag foil (blue line). A green line shows the high-energy edge (6.5 keV) for the linear Thomson scattering.

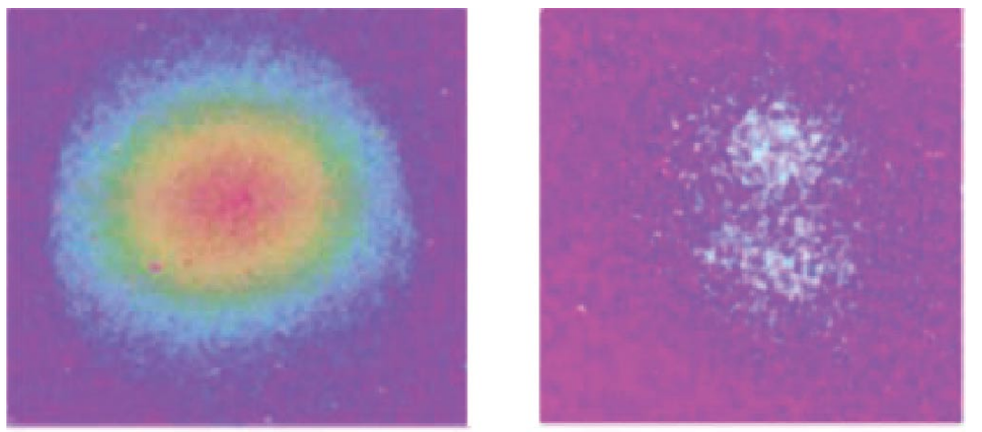

(a) (b) with the Ag foil

FIG. 3 (color). X-ray images observed on a luminescent screen: (a) without the Ag foil, and (b) with the 10 μm Ag foil filter.

CAIN results

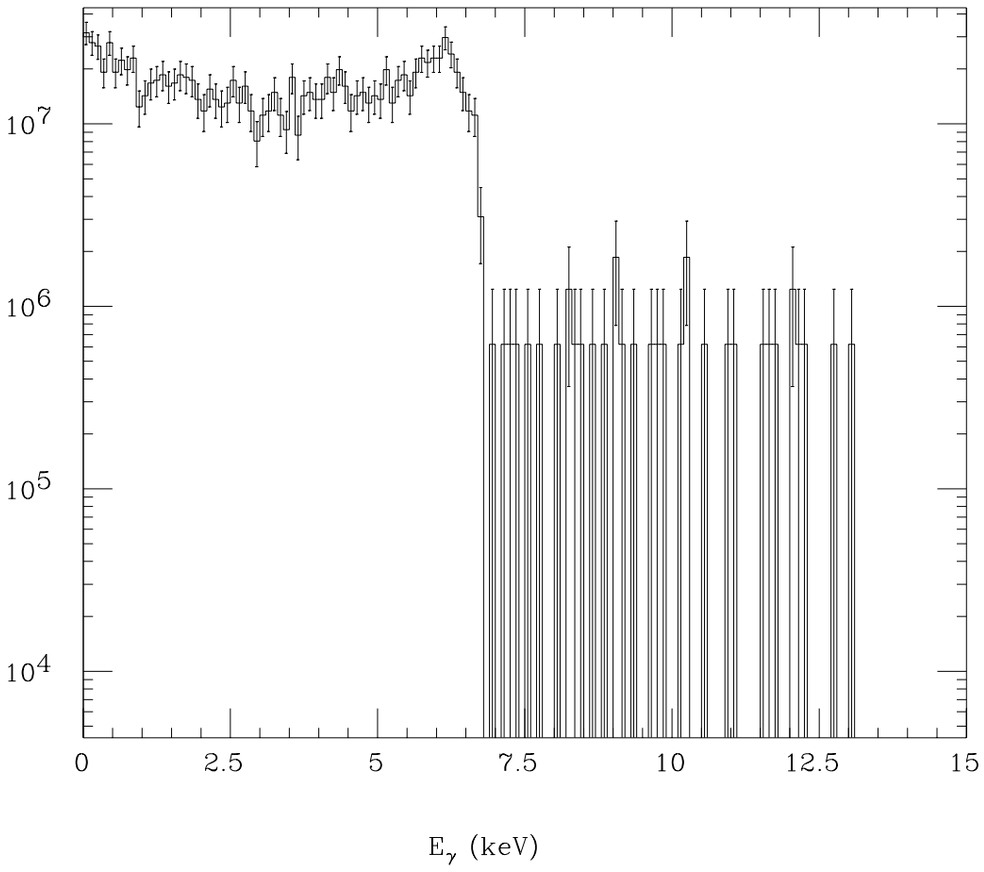

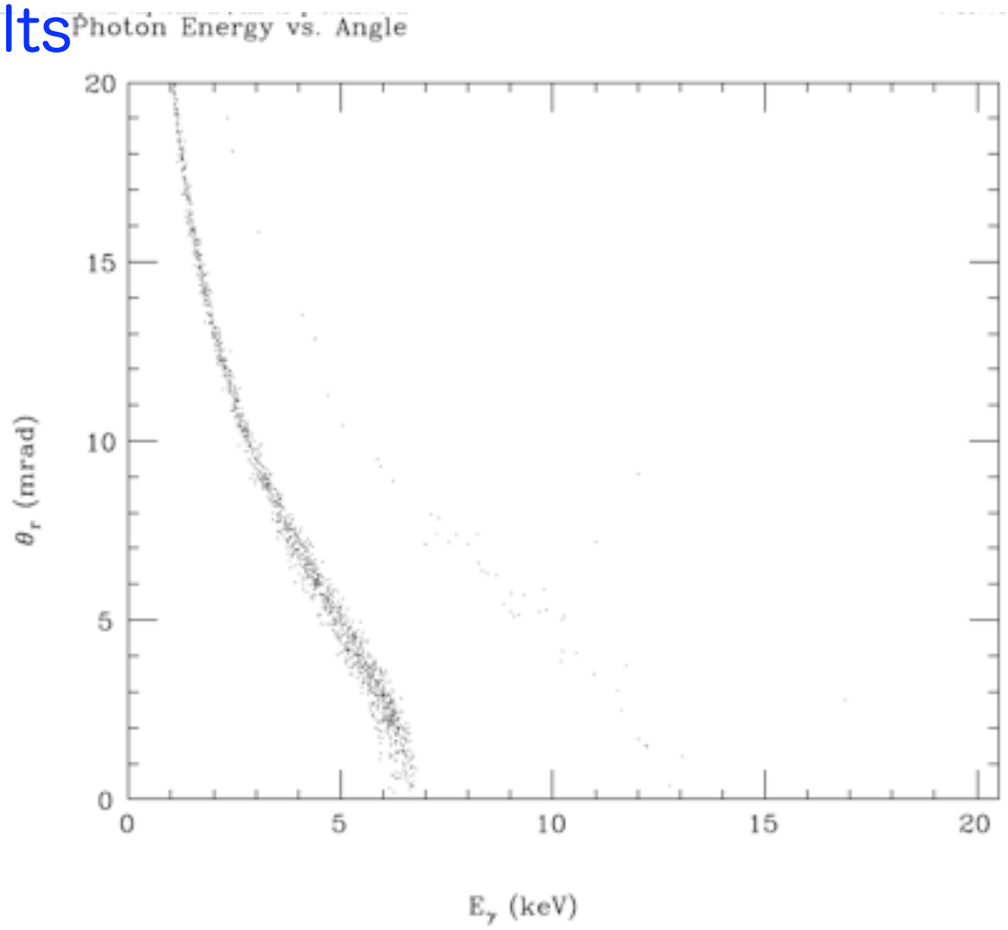

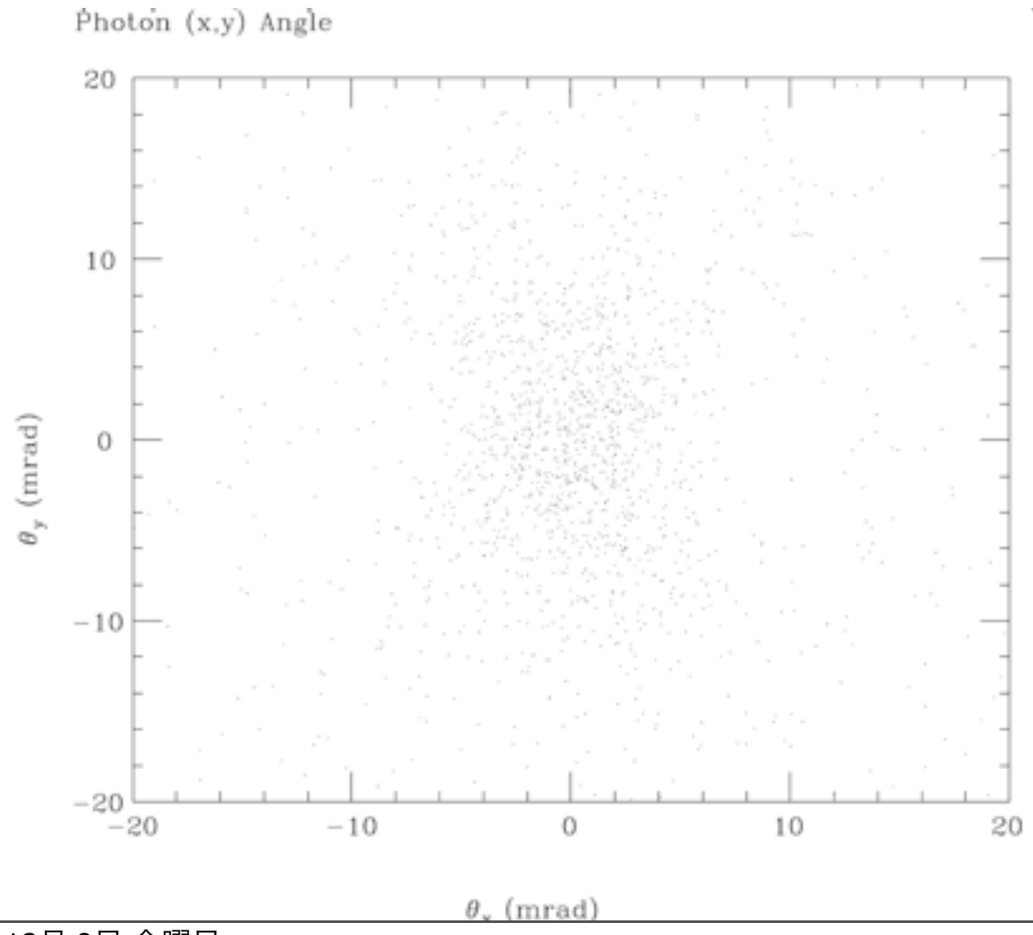

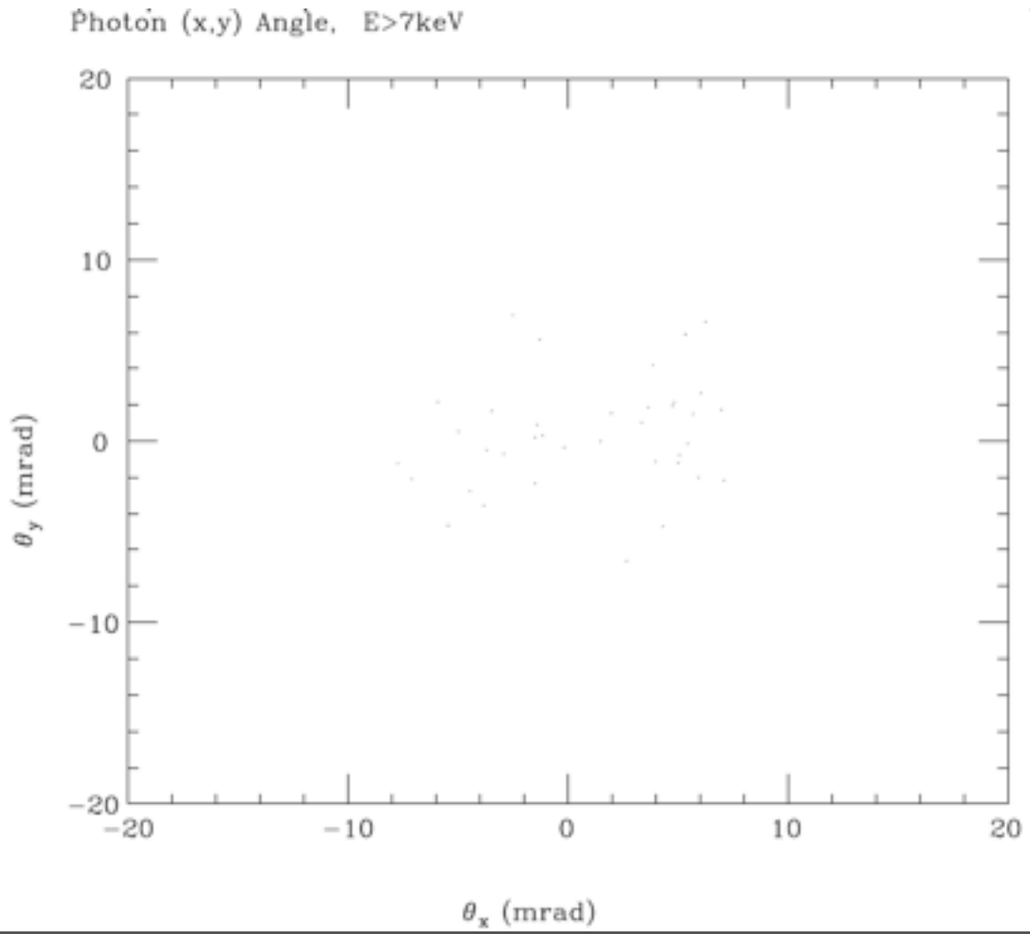

CAIN results of BNL 2nd stage

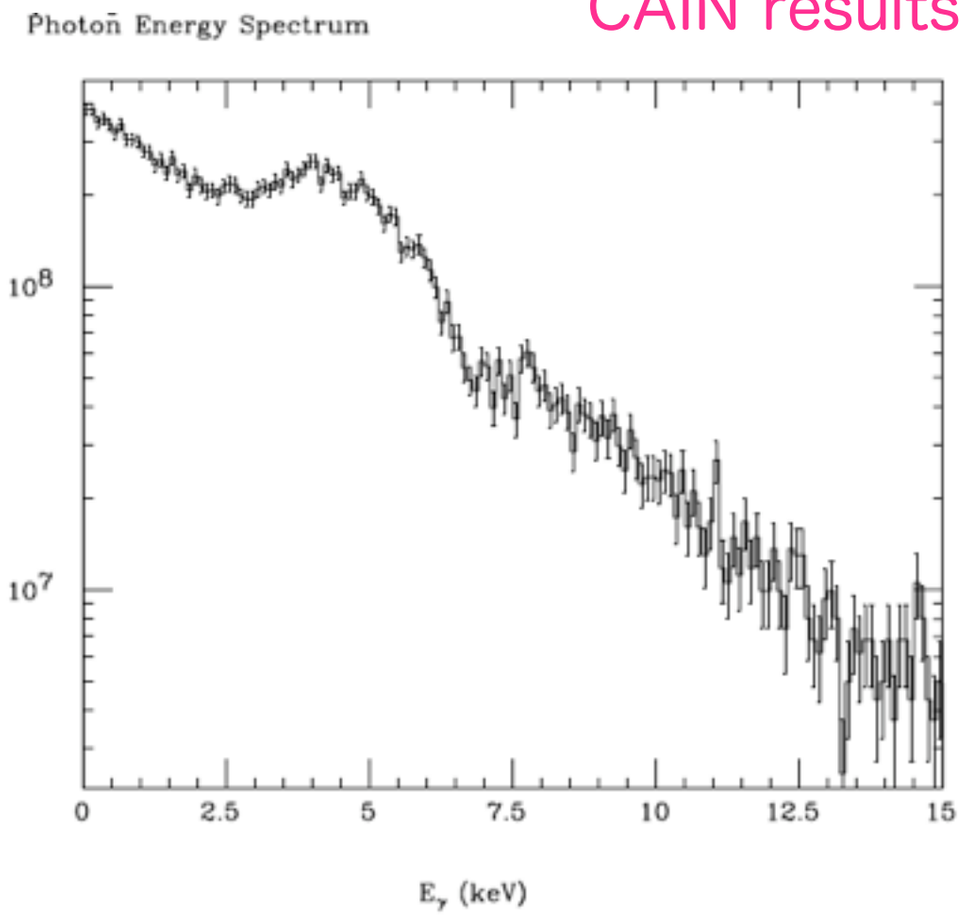

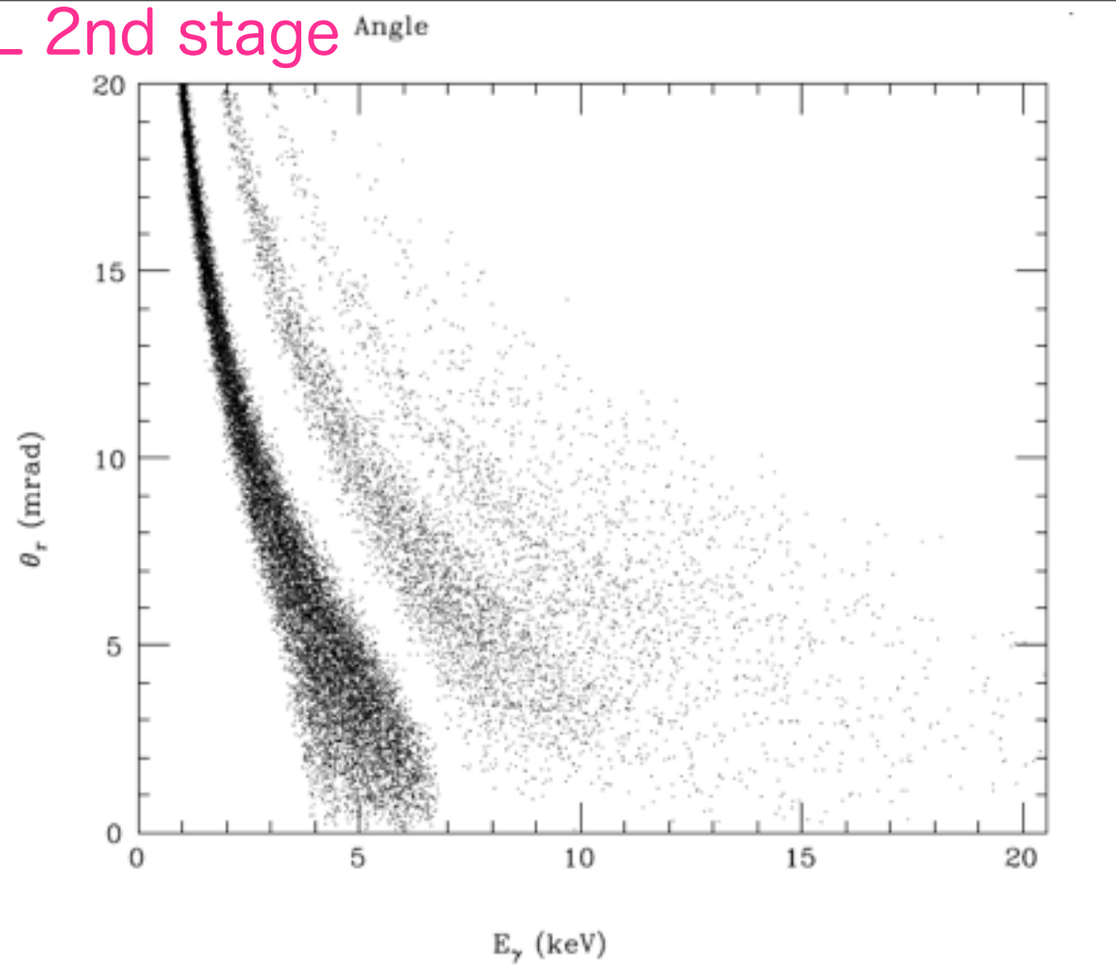

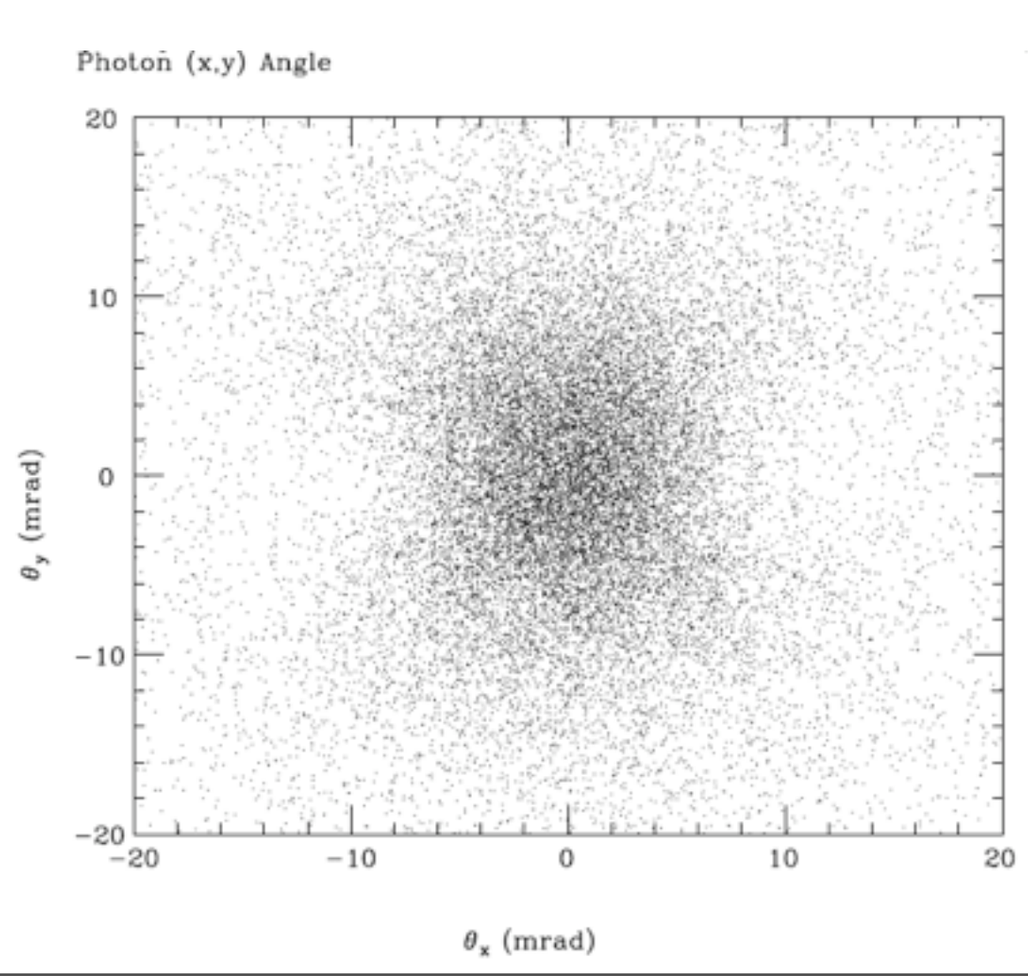

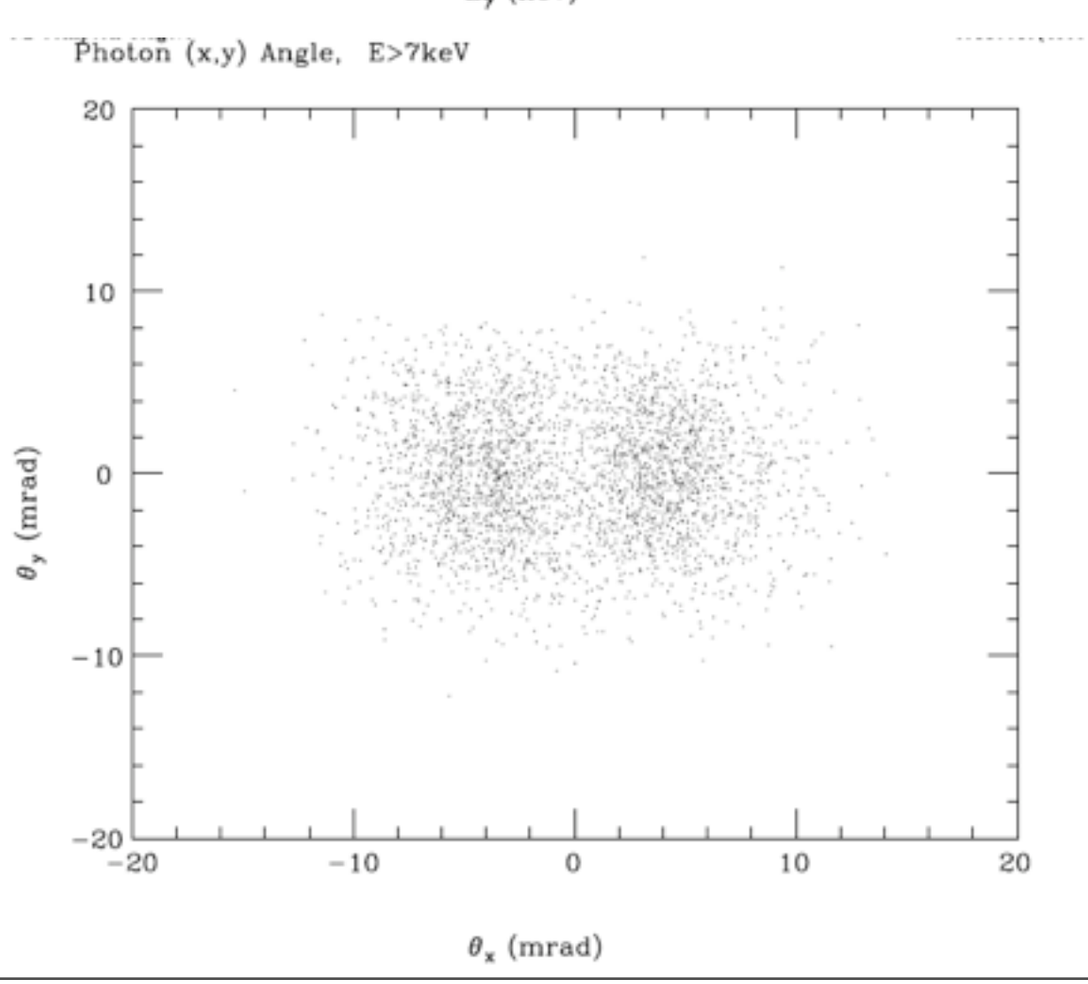

SLAC experiment, PR D60, 092004(1999), PRL 76, 3116 (1996)

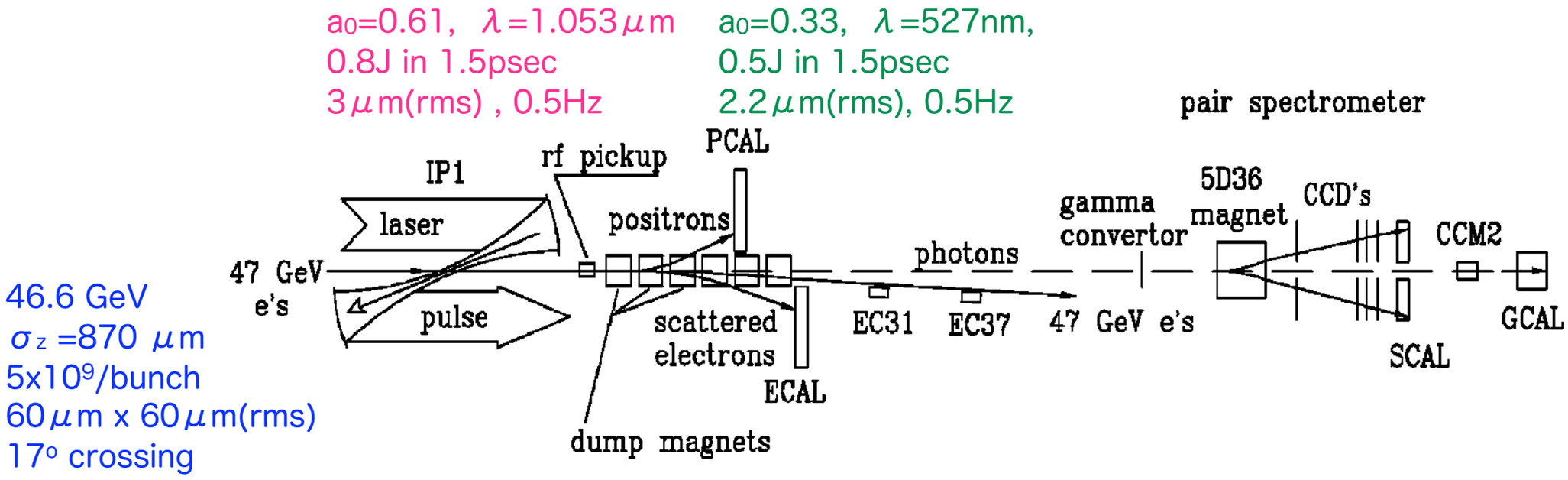

FIG. 11. Schematic of the experimental setup: The laser pulses crossed through the electron beam at the interaction point, IP1. The scattered electrons were deflected by the dump magnets into the electron calorimeter (ECAL). Positrons were deflected into the positron calorimeter (PCAL). The scattered photons were detected in a Čerenkov counter (not shown), or converted to e^+e^- pairs which could be detected by the pair spectrometer.

Compton scattering with Infrared laser $e + n\omega \rightarrow e' + \gamma$

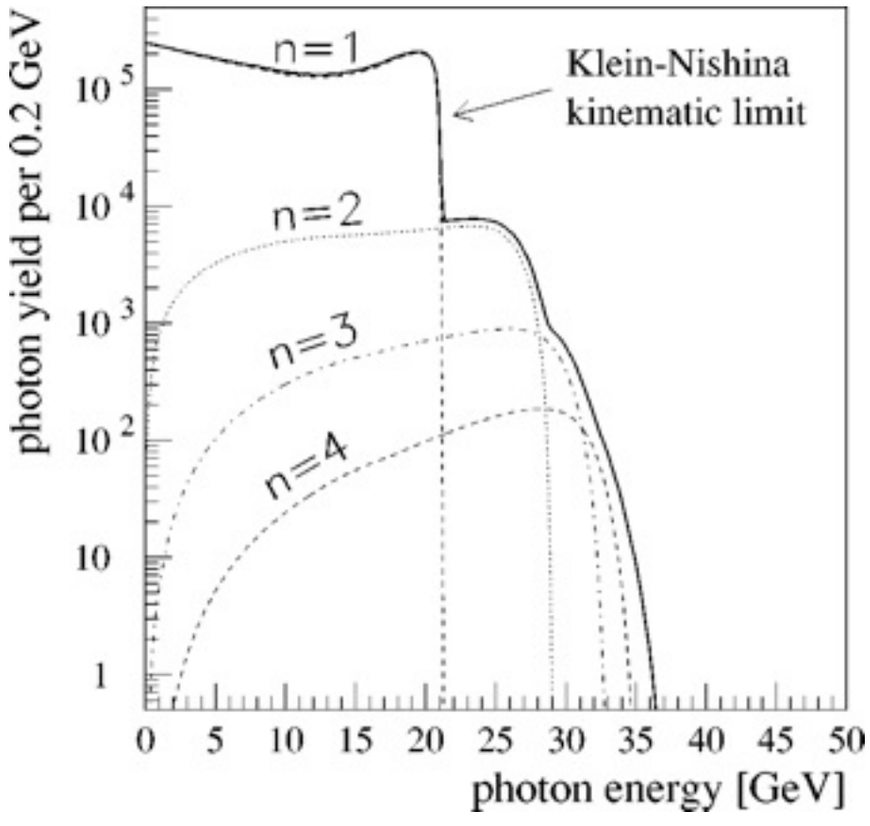

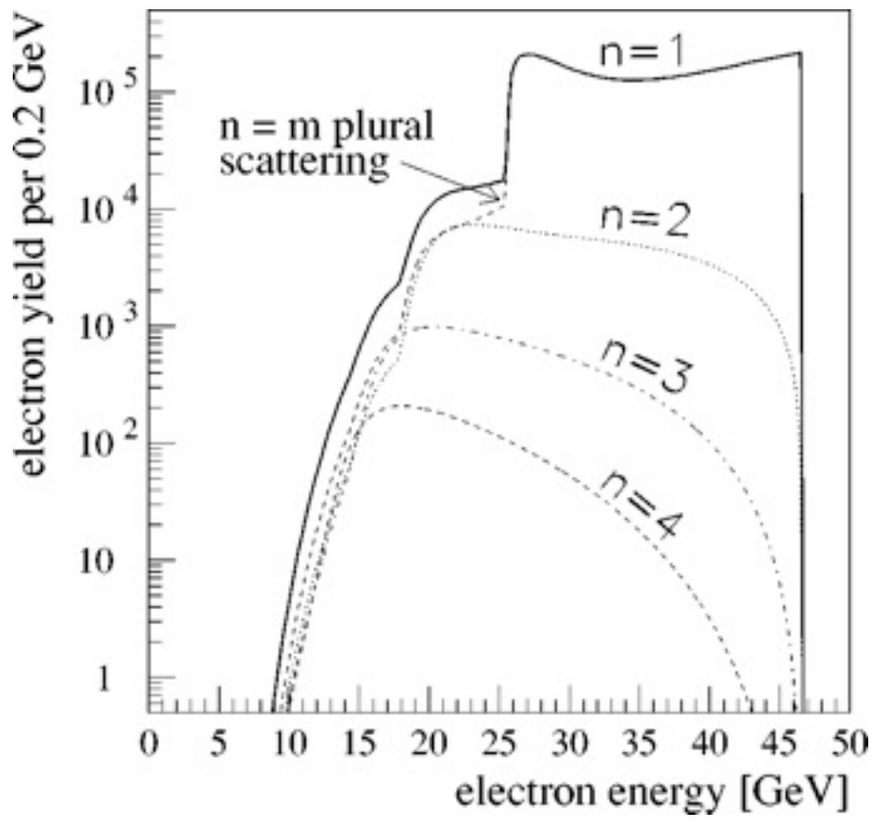

The yield of nonlinearly scattered electrons vs momentum P

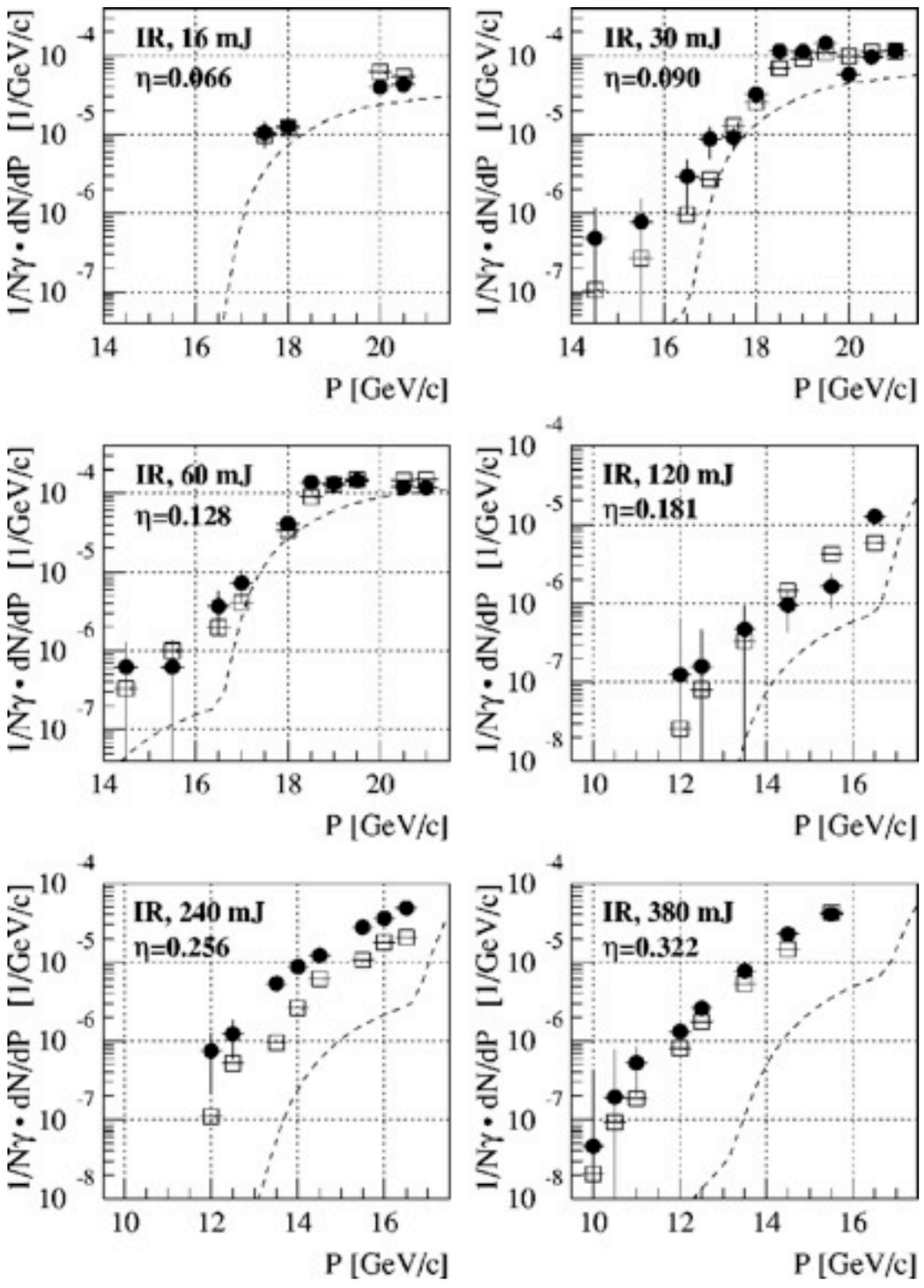

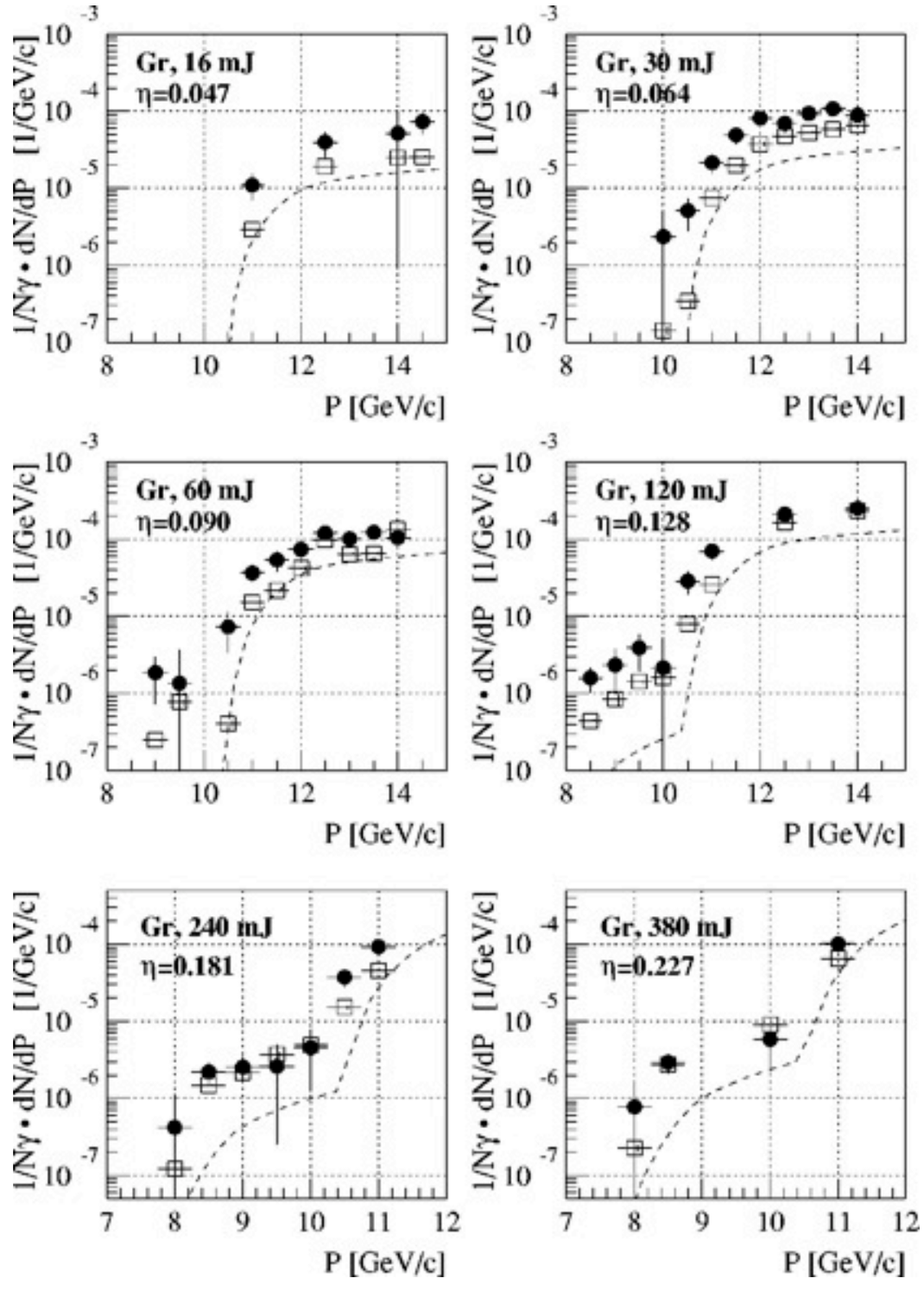

The data are the solid circles with vertical error bars corresponding to the statistical and reconstruction errors added in quadrature. The open circles are the simulation. The dashed line is the simulation of n=m plural scattering.

The scattered electron yield

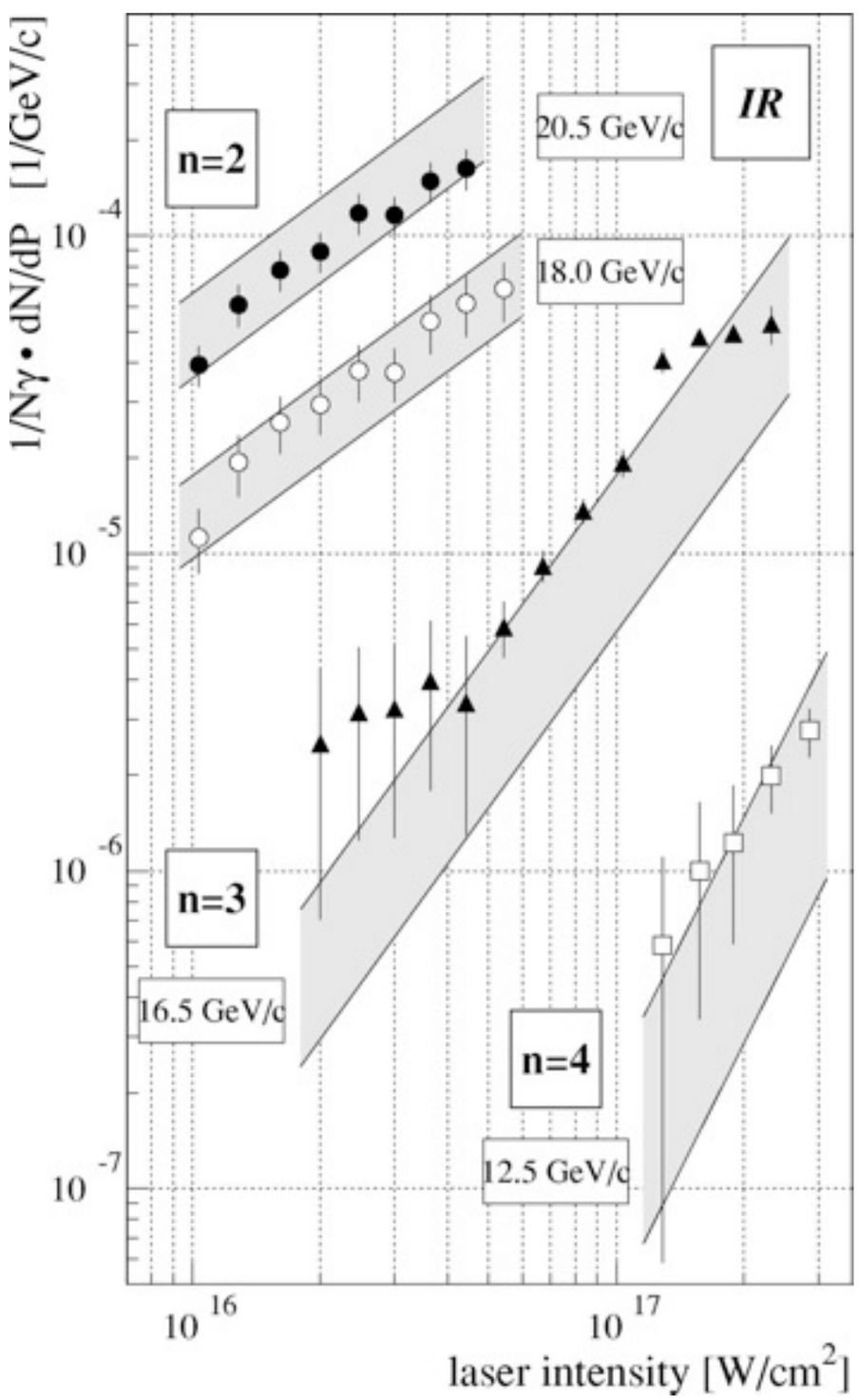

The simulation for each data set is shown as bands representing the 30% uncertainty in the IR laser intensity.

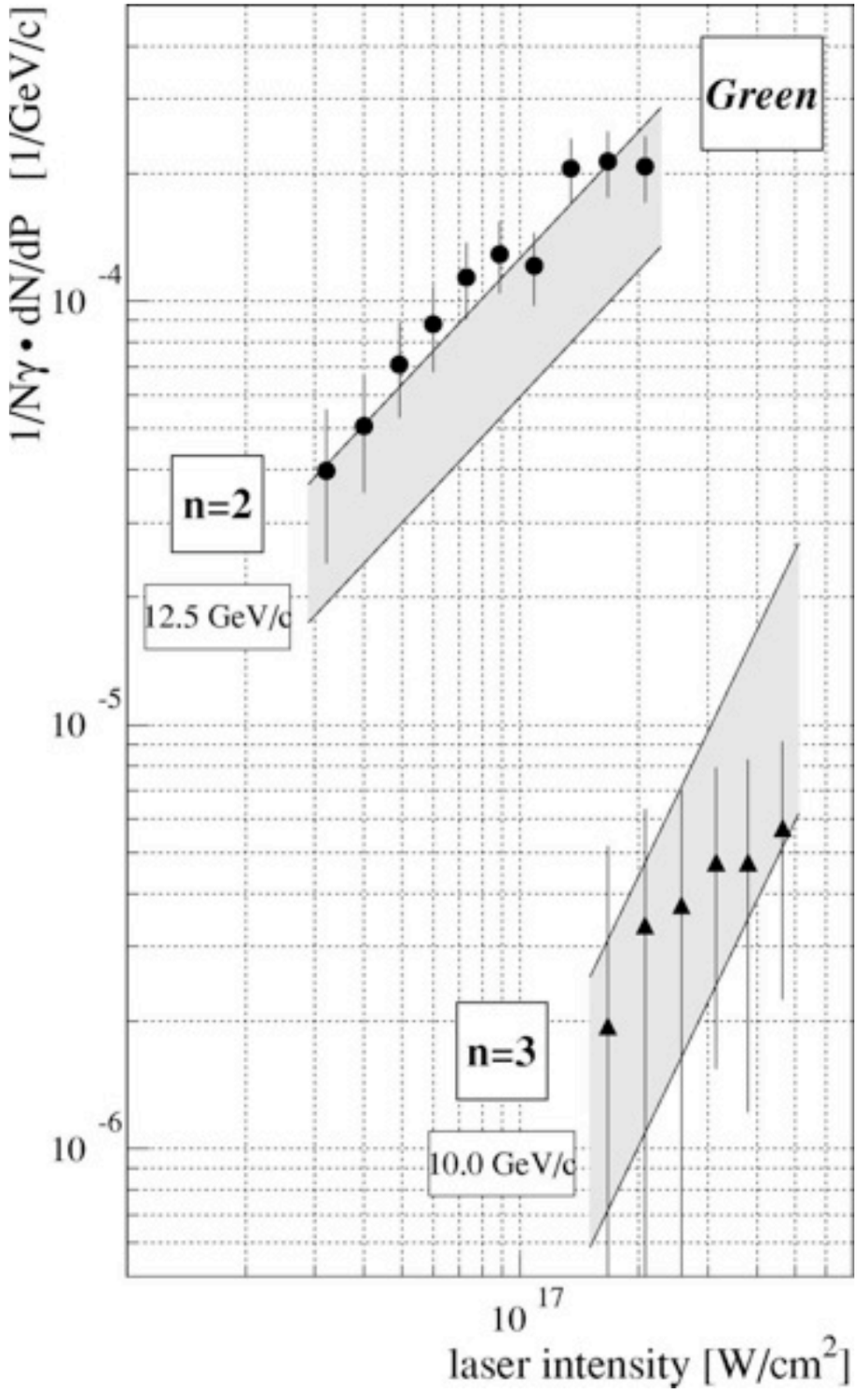

The simulation for each data set is shown as bands including the +50%, -30% uncertainty in the laser intensity.

CAIN results for the IR laser, 0.8J/pulse

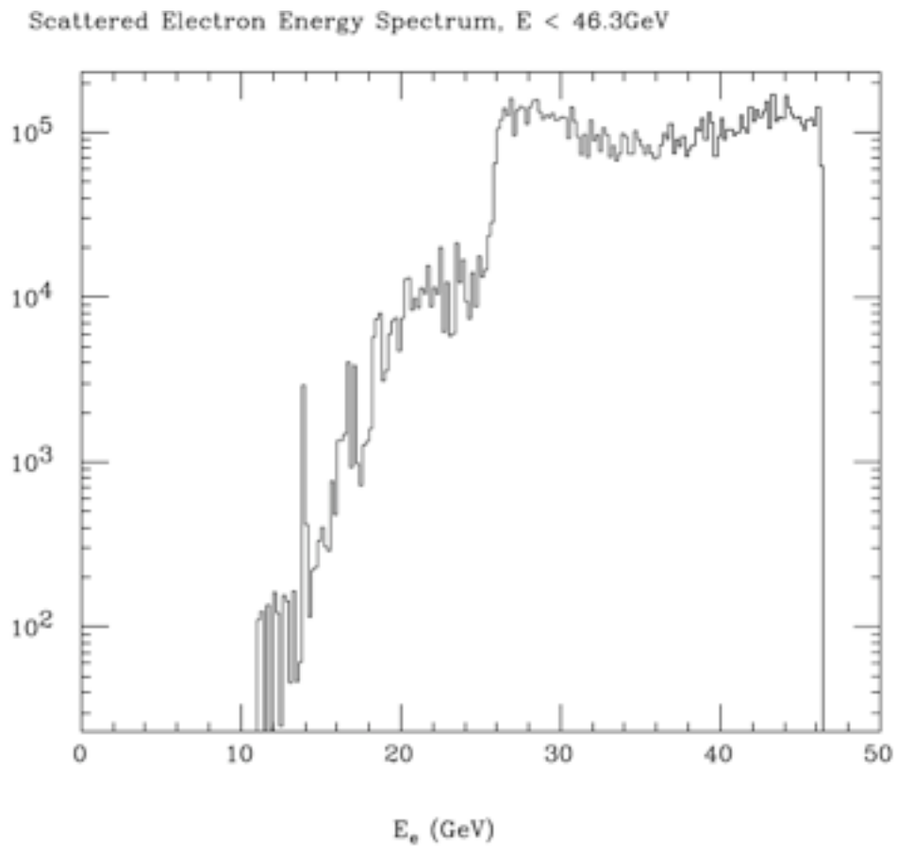

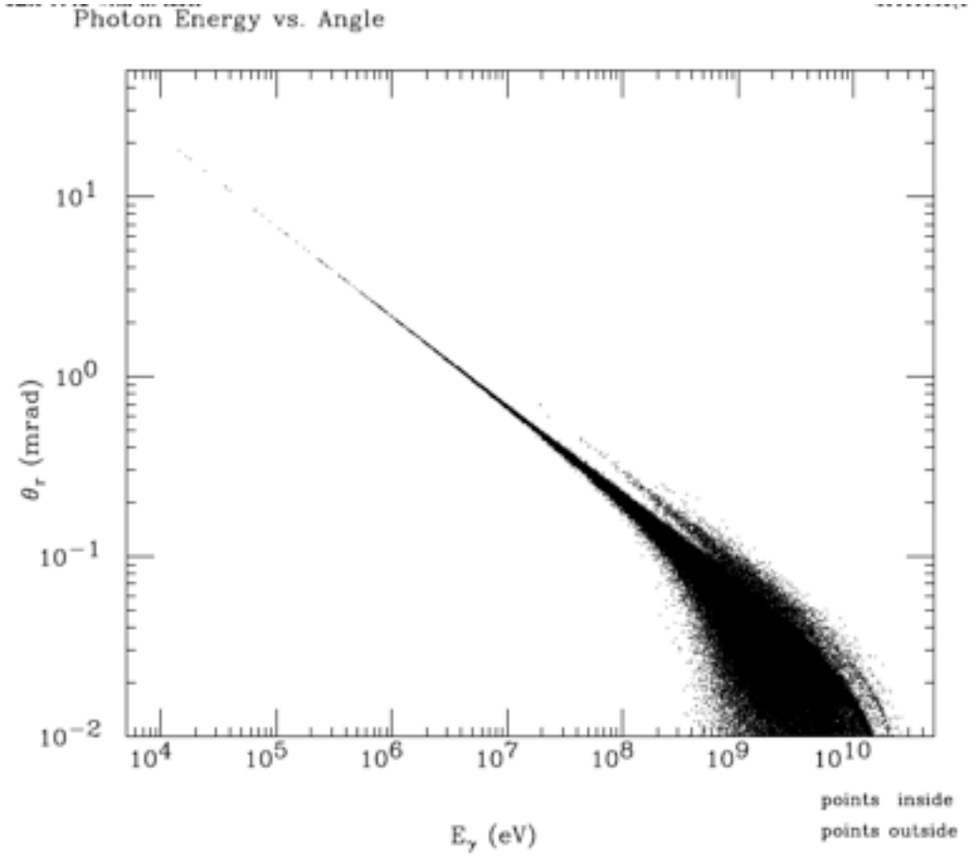

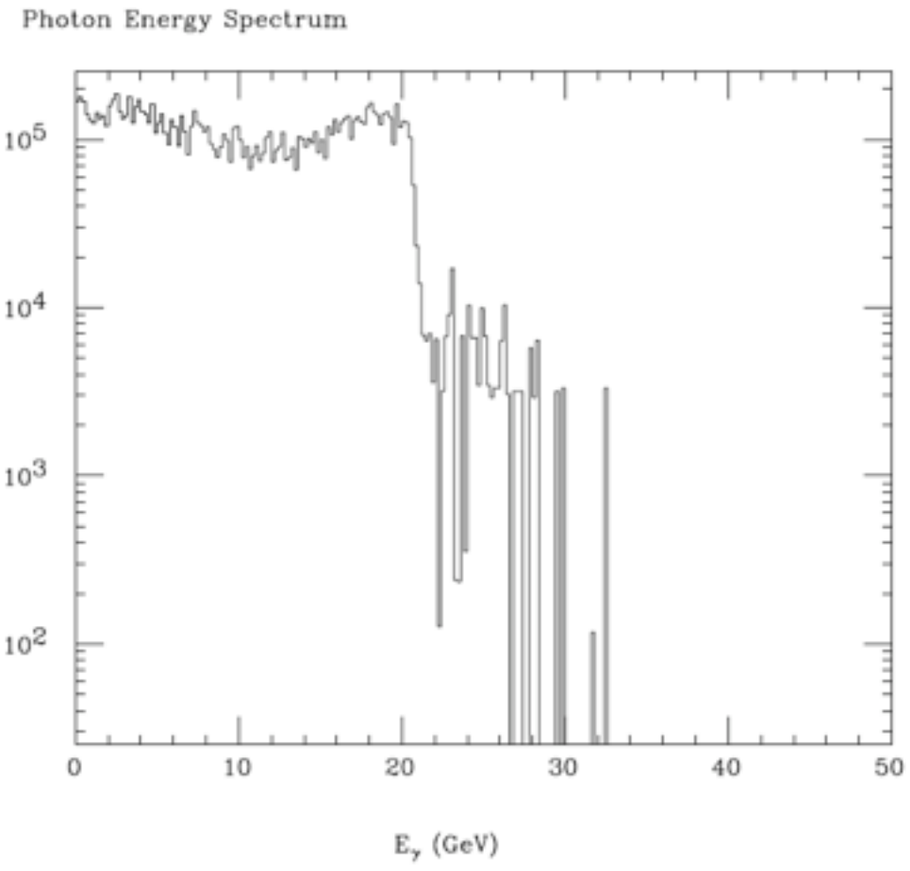

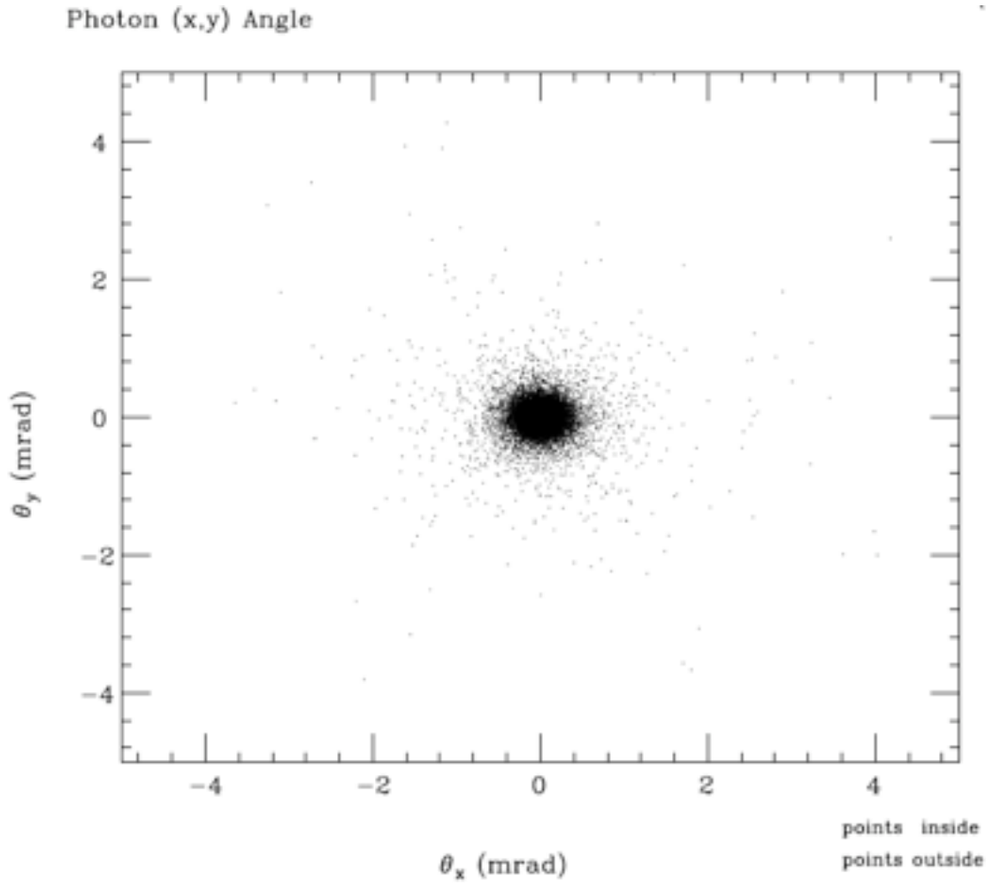

CAIN results for the green laser, 0.5J/pulse

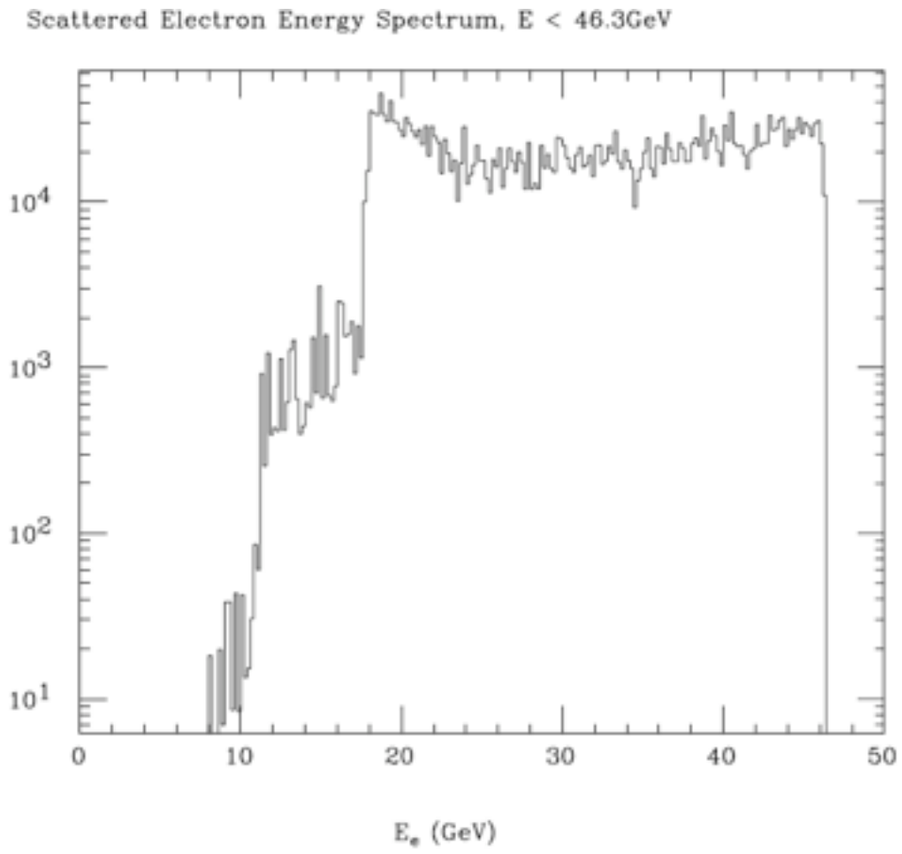

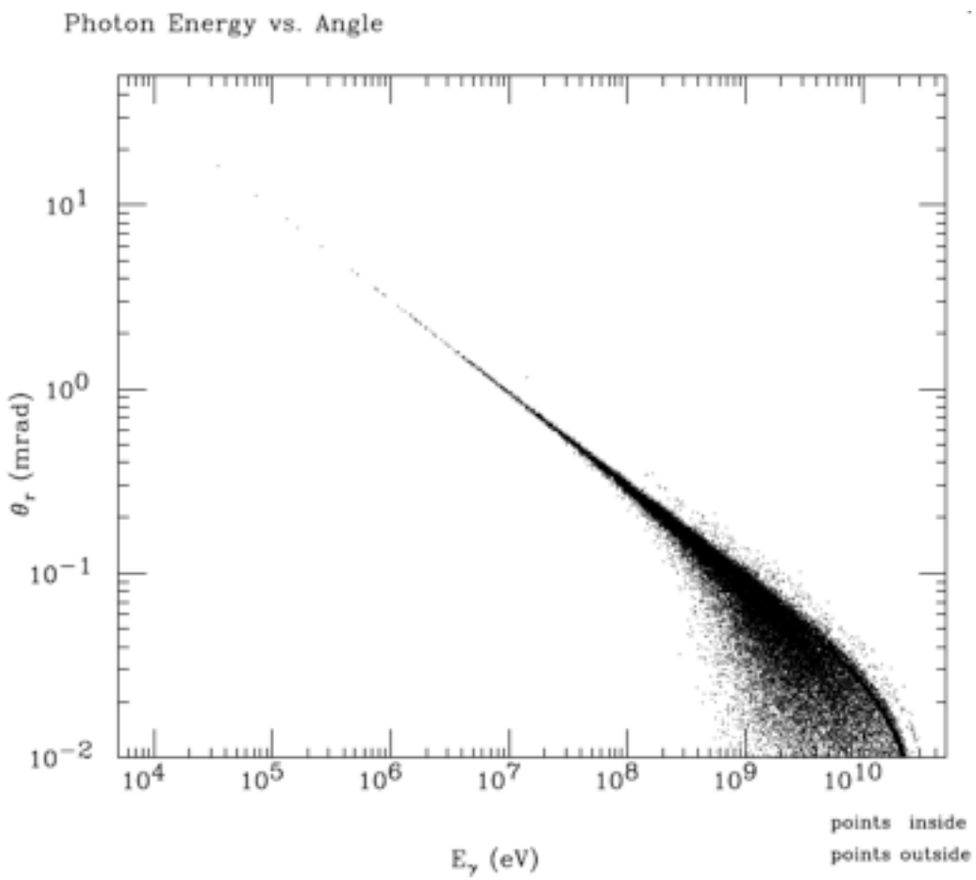

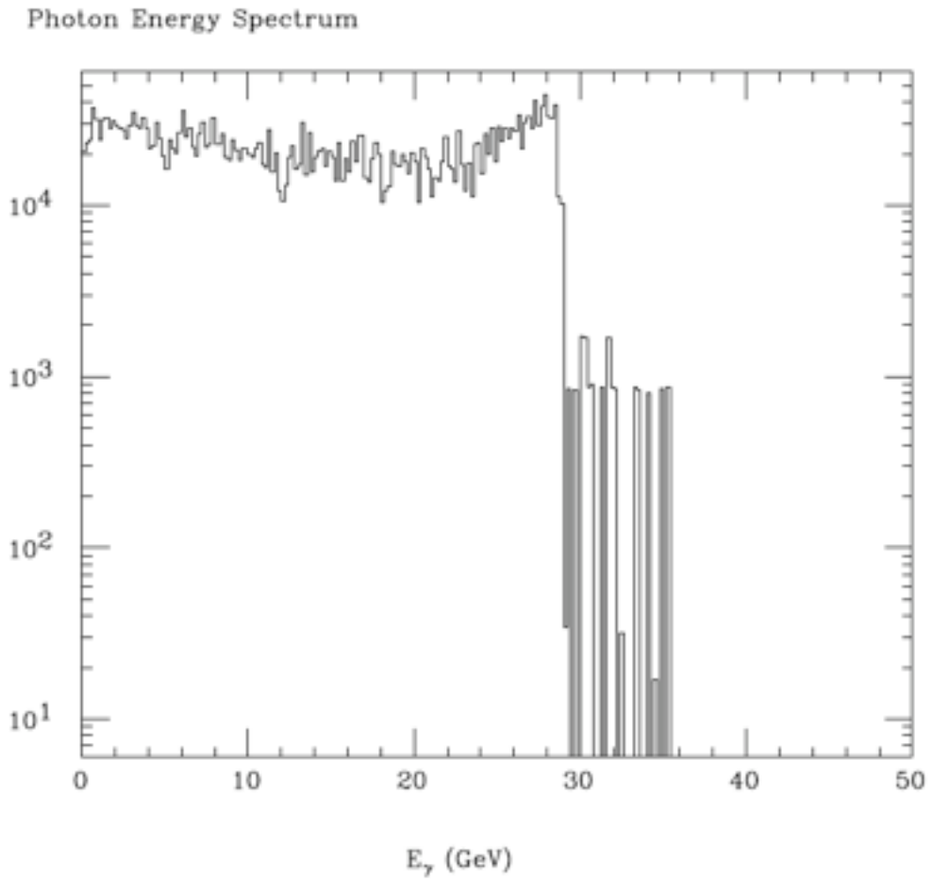

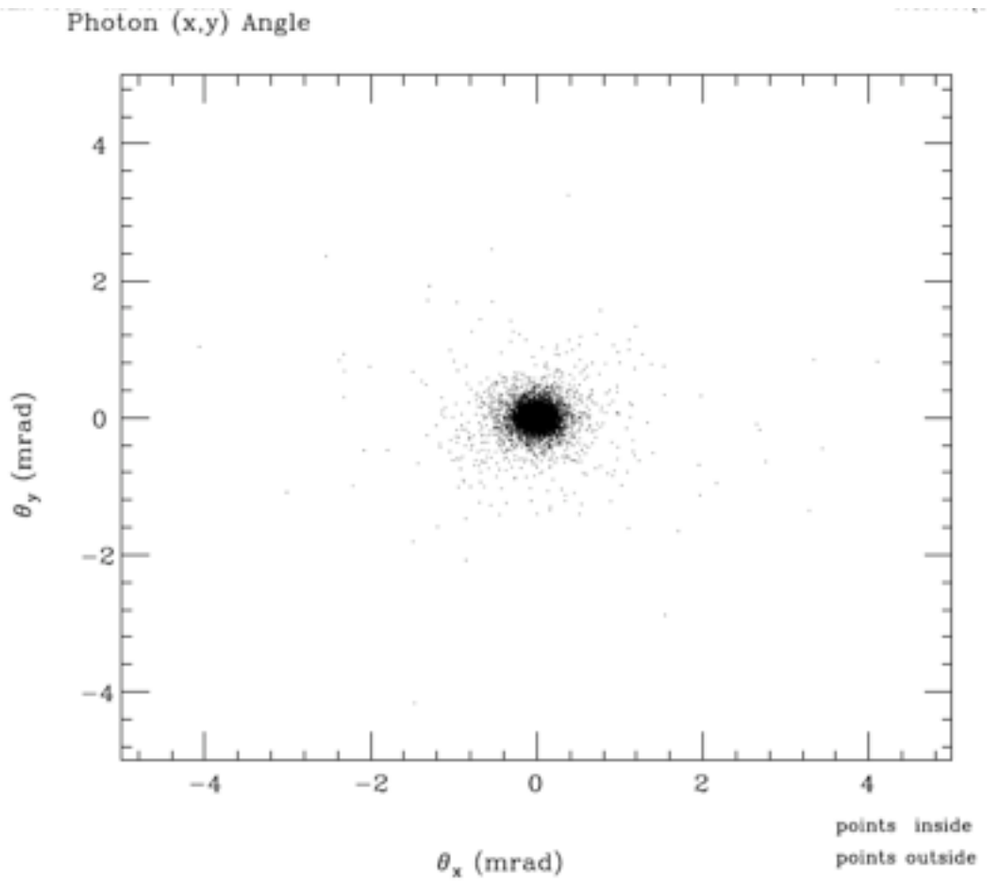

Positron productions $\gamma + n\omega \rightarrow e^+e^-$

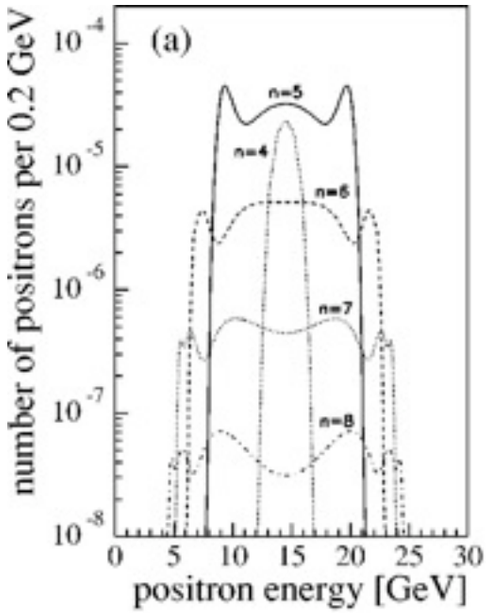

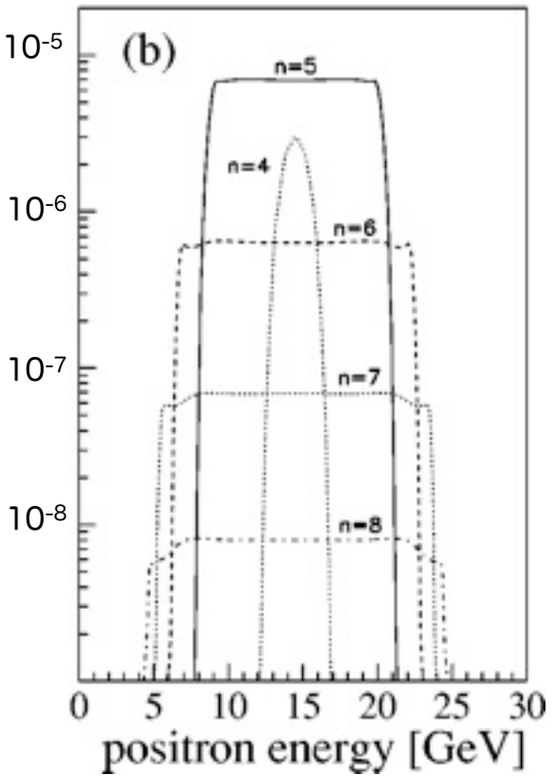

FIG. 8. Calculated energy spectra of positrons produced in the interaction of a 30 GeV photon with a 527 nm laser beam. (a) Parallel polarization. (b) Perpendicular polarization. The curves are labeled by the number of laser photons involved

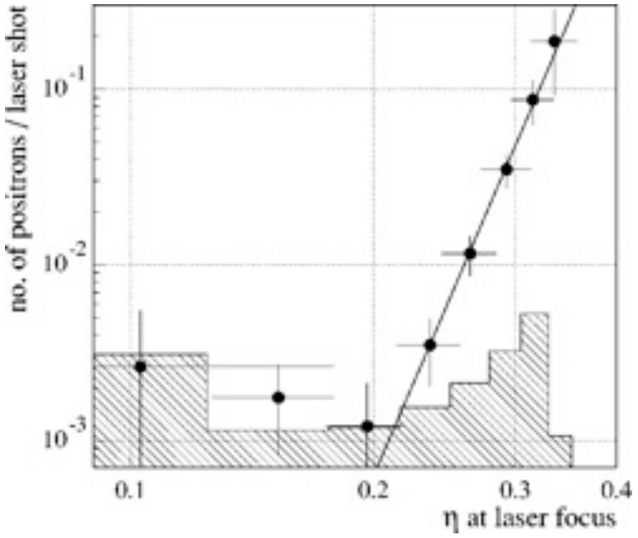

FIG. 44. The dependence of the positron rate per laser shot on the laser field-strength parameter η. The line shows a power law fit to the data. The shaded distribution is the 95% confidence limit on the residual background from showers of lost beam particles after subtracting the laser-off positron rate.

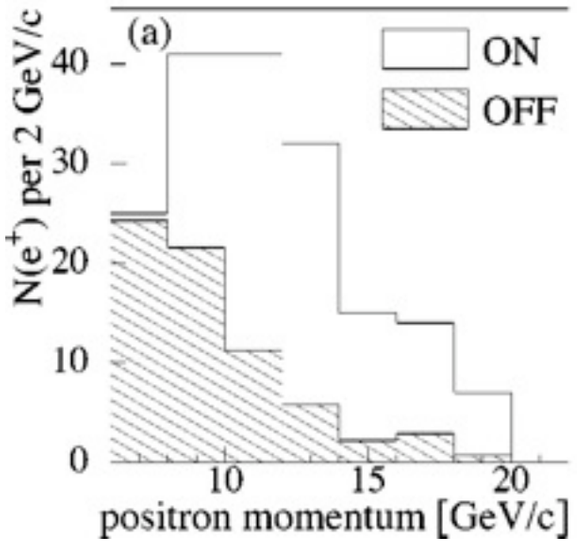

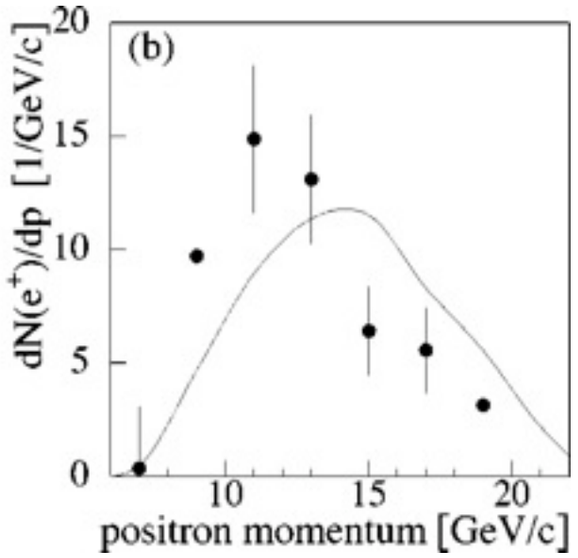

46.6GV electron beams and a linearly polarized green laser (0.5J), about 22,000 laser-on electron pulses, (b) 106±14 positrons

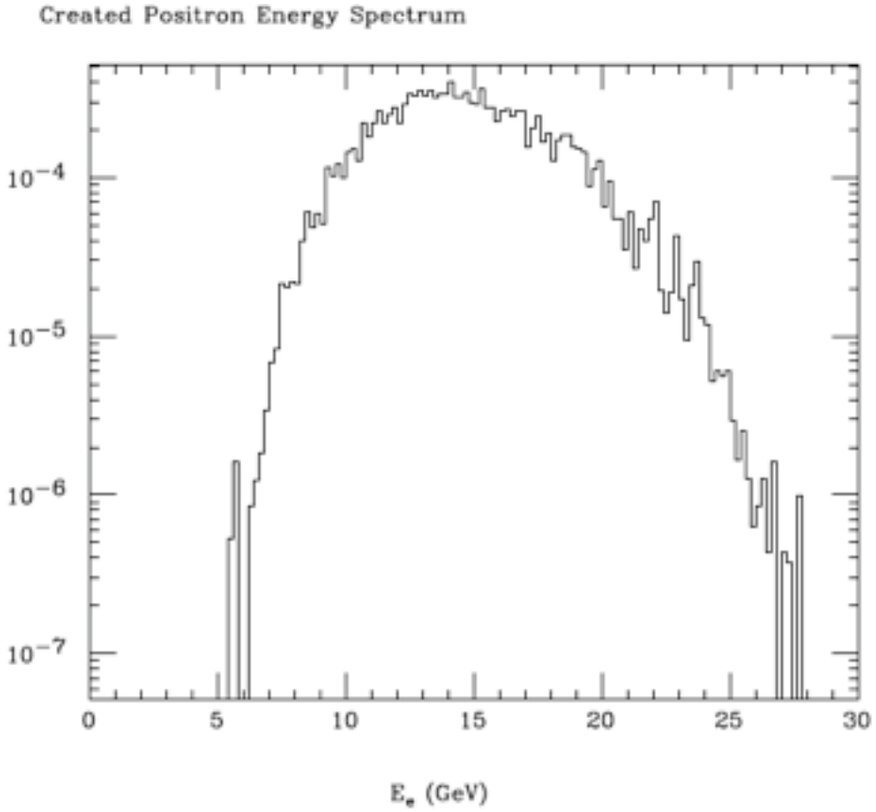

CAIN calculations with the circular polarized laser : 303 positrons generated with 22,000 pulses (1.38E-2/shot, a_0=0.33)

Brilliant hard γ-production and e^+e--creation in vacuum with ultra-high laser fields: Testing theoretical predictions at ELI-NP

Dietrich Habs, Peter Thirolf, Nina Elkina and Hartmut Ruhl
Fakultät für Physik, Ludwig-Maximilians-Universität München, D-85748 Garching, Germany

To study the "boiling of the vacuum" by a high intensity laser of
10^{24}W/cm^2, E=4.7 x 10^{15}V/m, a=10^3

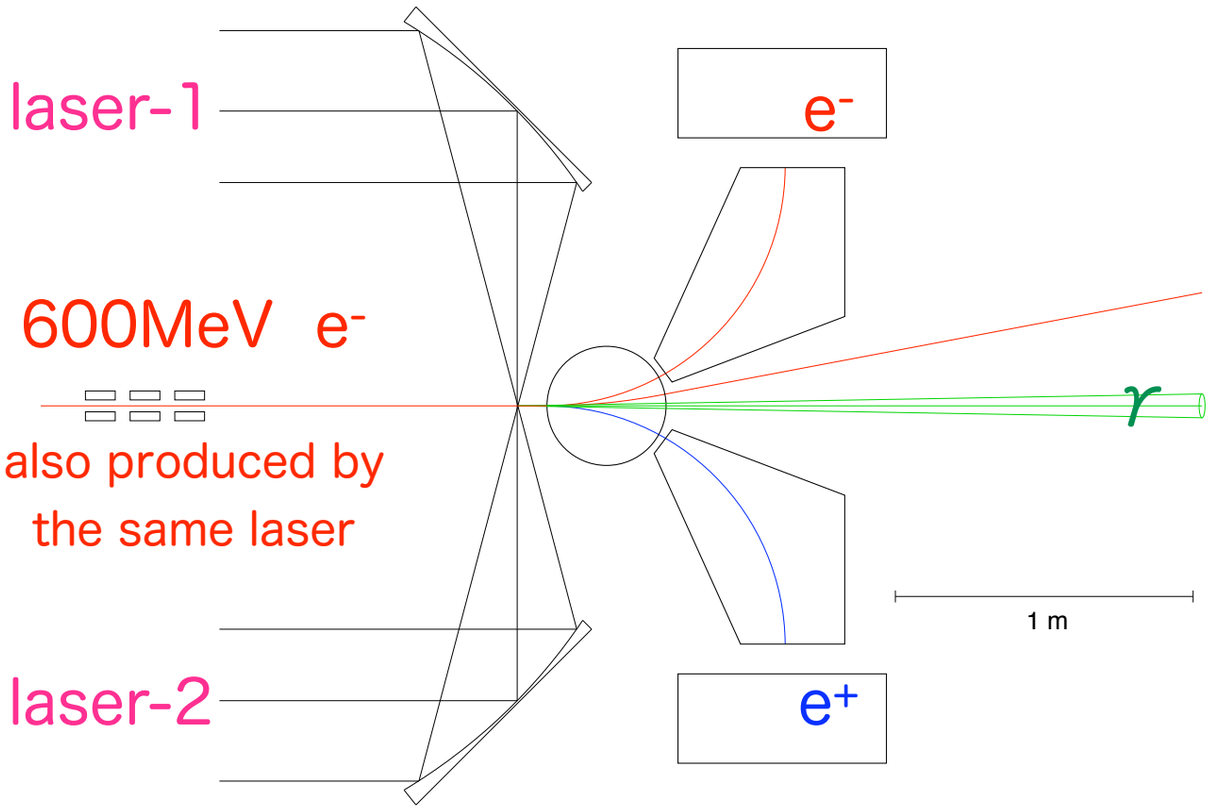

Figure 1: Experimental setup, showing the two focusing mirrors with the high-field focus and the triplet lense which focusses the electron beam (red) into the laser focus. Behind the laser focus, a dipole magnet deflects the electron beam, while the γ beam (green) continues straight on.

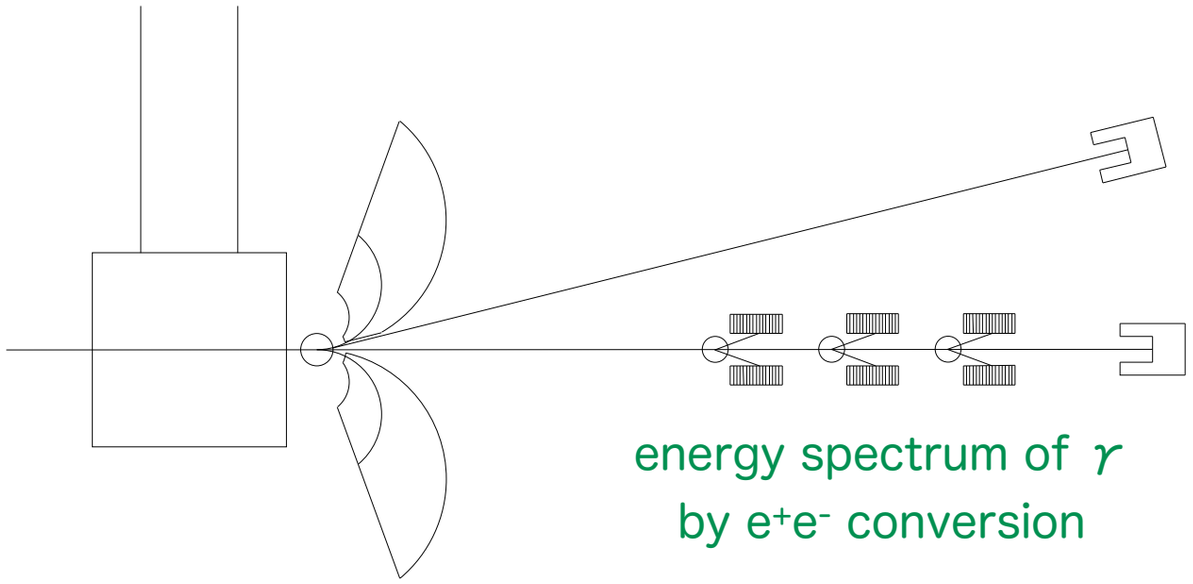

Figure 2: Extended view of the experimental setup, showing the sampling measurements on the γ beam, where in thin foils γ-quanta are converted to e^+e^- pairs, which then are deflected in small magnets and measured in calorimeters.

Two oppositely circular polarized lasers can create B=0, .e. only E field at crossing point

$$F = -\frac{F_{\mu\nu}F^{\mu\nu}}{2E_s^2} = \frac{\vec{E}^2 - c^2\vec{B}^2}{E_S^2}$$

$$G = \frac{\epsilon_{\mu\nu\lambda\kappa}F^{\mu\nu}F^{\lambda\kappa}}{8E_S^2} = \frac{c\vec{E}\cdot\vec{B}}{E_S^2}$$

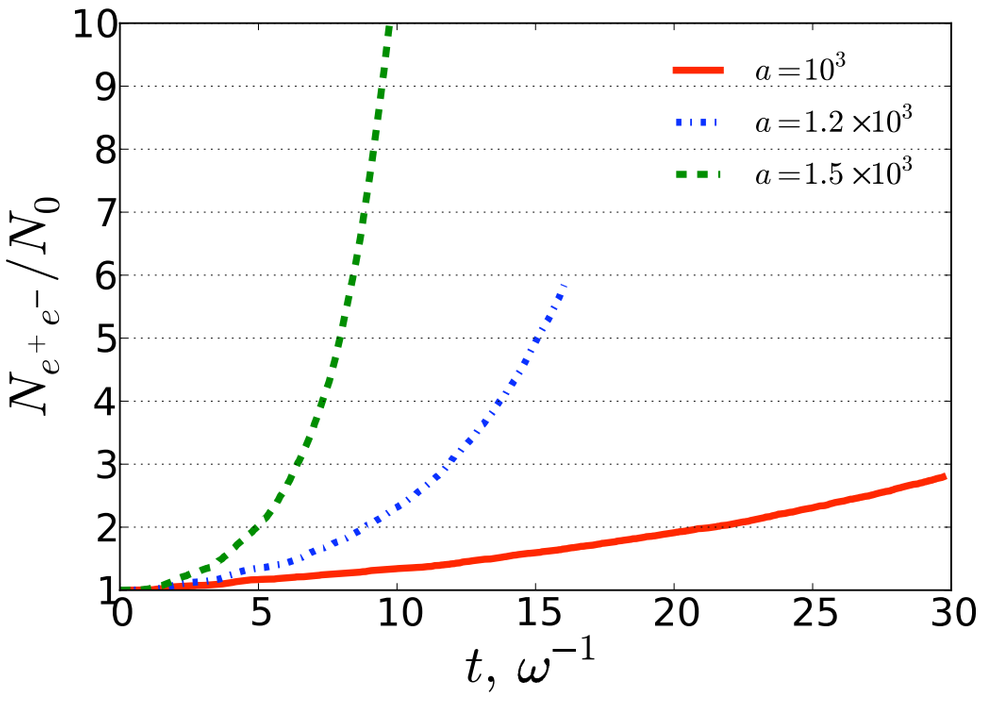

Figure 3: Simulated yield of electron positron pairs as a function of time for different values of the dimensionless field amplitude $a = 10^3,\ 1.2 \times 10^3,\ 1.5 \times 10^3$. The energy of the primary electron beam is $600 MeV$.

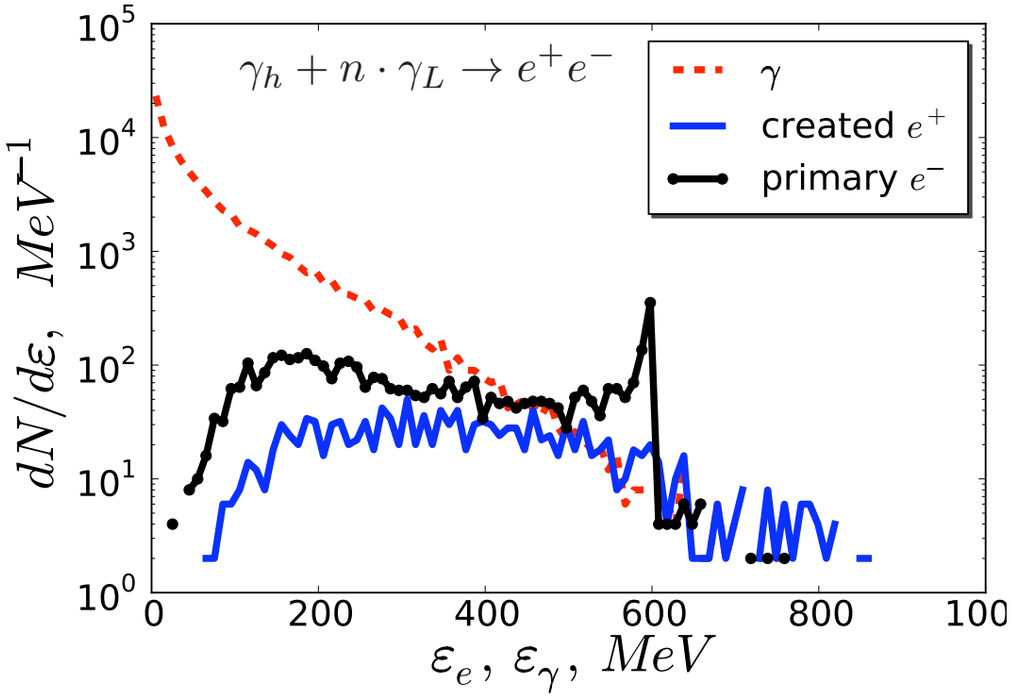

about 20 γ's and about 2 e^+e^- pairs/shot

Figure 4: Simulated spectra of generated γ-quanta, positrons and electrons for a focus with a rotating E field and 10^{24}W/cm^2 and a 600 MeV electron bunch.

Table 1: Comparison of the parameters of the ELI-NP and E144 SLAC experiments [12]

QED cascades

parameter	ELI-NP	E144 SLAC
norm. vec. potent. a	1000	0.36
laser intensity	$\approx$ **10^{24}**W/cm^2	**$1.3 \cdot 10^{18}$**W/cm^2
laser width	15 fs	1600 fs
σ_x	$\approx$ **1**μm	**25**μm
σ_y	$\approx$ **1**μm	**40**μm
E_e	0.6 GeV	46.6 GeV
N_e	1.5·**10^9**e	7·**10^9**
repetition rate	0.02 Hz	10-20 Hz
χ_e	1.7	0.3
χ_γ	$\approx$1	0.2
photons absorbed in pair cr. n_{pair}	$\approx$ **10^9**	$\approx$ **5**

QED IN ULTRA-INTENSE LASER FIELDS

TOM HEINZL
PIF2010, KEK, TSUKUBA

24 NOVEMBER 2010

With: N. Iji, K. Langfeld (UoP), C. Harvey, A. Ilderton, M. Marklund (Umeå), A. Wipf (Jena), H. Schwoerer (Stellenbosch), B. Kämpfer, R. Sauerbrey, D. Seipt (FZD)

Modelling a laser

- In order of increasing complexity:
  - Plane wave ☑
    - Infinite (IPW)
    - Pulsed (PPW)
      - Finite T-duration
      - Infinite transverse extension

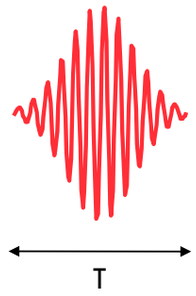

  - Gaussian beam: ☒
    - Finite transverse waist w
    - Finite longitudinal extension z_0

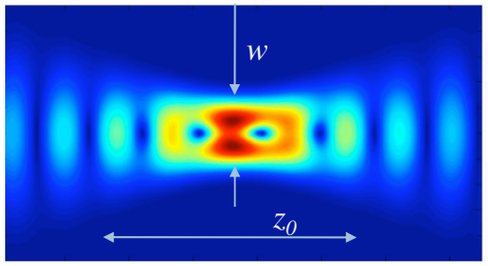

Charge in IPW

IPW : Infinite Plane Wave

- Solution of Lorentz force eq.: rapid quiver motion (momentum $p(\tau)$)
- Charge acquires **quasi-momentum**

$$q \equiv \langle p \rangle = p_{\text{in}} + \kappa(a_0^2)\, k$$

- Longitudinal addition – consequence:
- **Effective mass** squared

$$q^2 = m^2(1 + a_0^2) \equiv m_*^2$$

- *The* basic intensity effect!

(Sengupta 1951, Kibble 1964)

Charge in pulsed PW

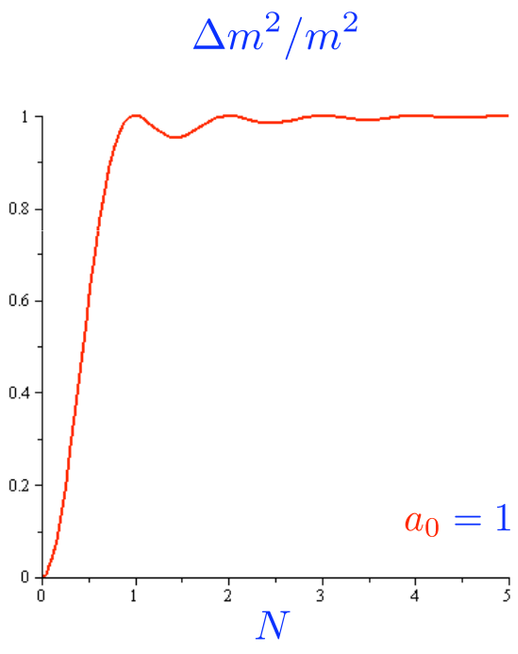

Kibble, Salam, Strathdee 1975

- Volkov propagator →
  - Mass shift Δm^2 depends on pulse duration, T
  - gradually builds up with number of cycles per pulse, N →
  - **Finite** (temporal) **size effects**
  - **NB:** ultra short pulses

$$T \sim O(1...10) \text{ fs}$$
$$N \sim O(1)$$

Strong-field QED

- Probe photons

- Volkov sol^{n} of Dirac eq^{n} in *PW* field (Volkov 1935)
- Electrons 'dressed' by laser photons (---------)
- 'Volkov electron':

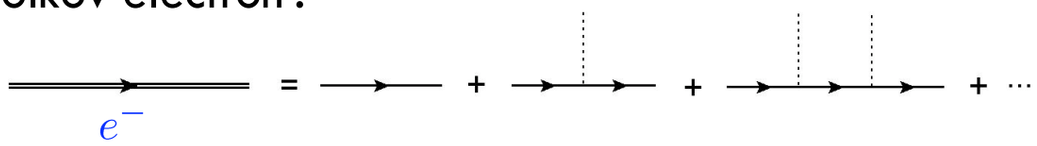

- Build transition amp^{s} between Volkov electrons from Feynman rules (`Furry picture')

NLC scattering

- Expand Furry picture Feynman diagram →
- Sum over all processes of the type $e + n\gamma_L \to e' + \gamma$

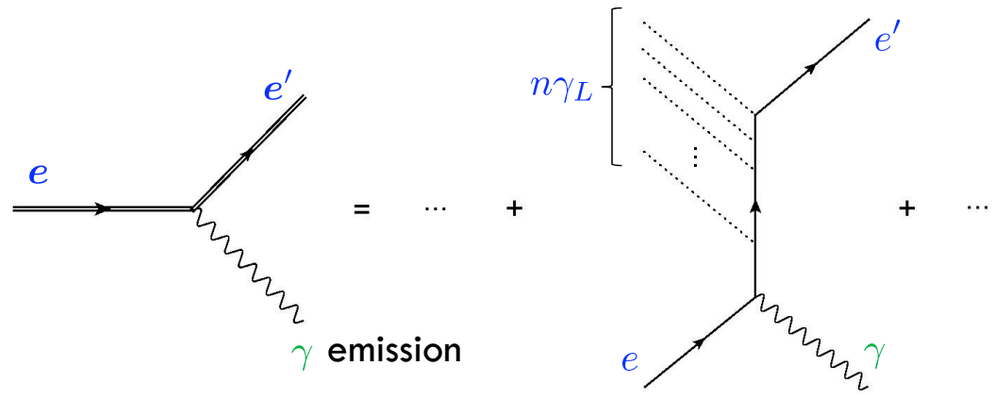

Schott 1912; Nikishov/Ritus 1964,
Brown/Kibble 1964, Goldman 1964

NLC cont^{d}

- For high intensity, $a_0 \gg 1$
- **modified** Compton edge

$$\omega'_{n,\mathrm{max}} \simeq 4\gamma_e^2 n\omega/a_0^2 \,, \quad n = 1, 2, \ldots$$

- In particular:
  - Higher harmonics: $n > 1$ ('nonlinear')
  - Overall blueshift maintained as long as $a_0 \lesssim 2\gamma_e$
  - **Redshift** of n=1 edge

$$\omega'_{\mathrm{max}} \simeq 4\gamma_e^2\omega \longrightarrow 4\gamma_e^2\omega/a_0^2$$

NLC spectrum: main a_0 effects

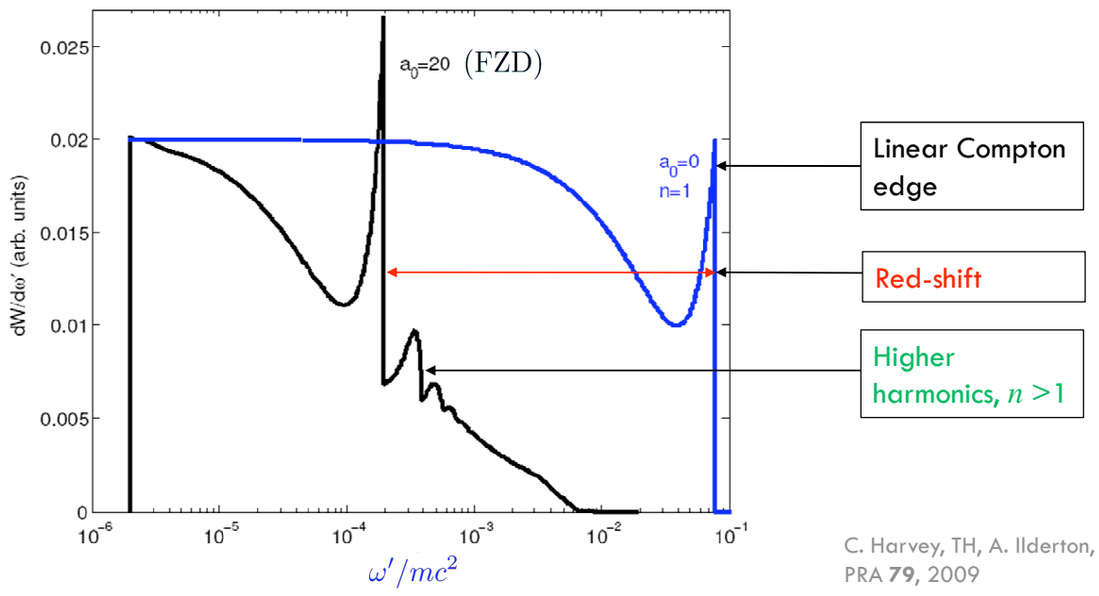

C. Harvey, TH, A. Ilderton,
PRA **79**, 2009

a_0 dependence (lab)

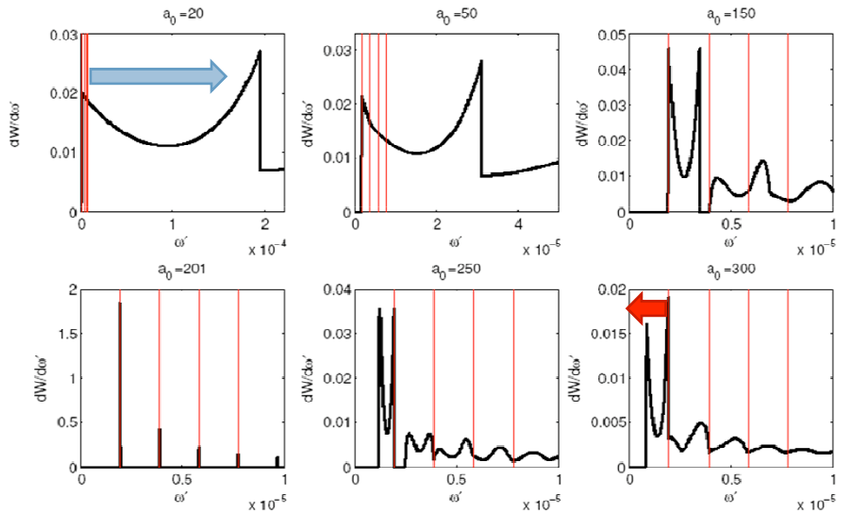

Tuning a_0 similar to changing frame: when $a_0 = a_{0c} \simeq 2\gamma$

'inverse' Compton → Compton

C. Harvey, TH, A. Ilderton, PRA **79**, 2009

Finite Size Effects

Strongly focussed: $w_0 < r_b$

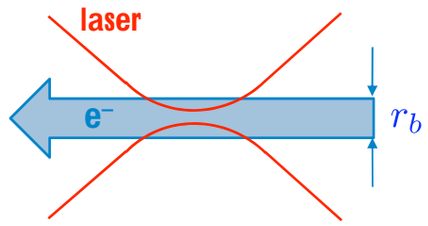

$a_0 \gg 1$

Weakly focussed: $w_0 \gg r_b$

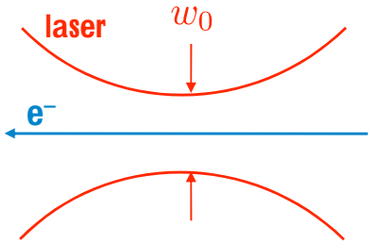

$a_0 = O(1)$

Vacuum birefringence (Brezin, Itzykson 1970)

Calcite crystal

- Two indices of refraction (Toll 1952)

$$n_\pm = 1 + \frac{\alpha\epsilon^2}{45\pi}\left\{11 \pm 3 + O(\epsilon^2\nu^2)\right\}\left\{1 + O(\alpha\epsilon^2)\right\}$$

- Dim.less (small) parameters:
  - Field strength: $\epsilon \equiv E/E_S$
  - Probe frequency $\nu \equiv \hbar\omega/mc^2$
  - fine structure const $\alpha = 1/137$

Conclusion

- Laser power approaching exawatt regime
- Extreme field physics – Schwinger limit: QED
- Experiments planned or under way
- X-ray generation: $a_0 = O(1)$
- Theory (→ a_0 dependence) :
  - Ok for plane wave models
  - Challenge: incorporate realistic laser beam model
    - Finite size effects
    - Beyond plane waves
    - Numerical approaches

Second order QED processes and their radiative corrections

Tony Hartin, PIF2010, 24 November 2010

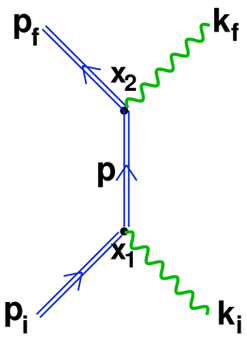

- Stimulated Compton Scattering (SCS)
- Bound state QED
- External circularly polarised/constant crossed electromagnetic fields
- Exact solutions of Dirac equation
- Resonances/Energy level widths/Vertex Correction

Why is SCS interesting?

- An electron in an external plane-wave, periodic field takes on an energy level structure

$$(p_i \pm sk)^2 = m^2 + e^2 a^2 \equiv m_*^2$$

- Modified conservation of momentum

$$\sum_{s=-\infty}^{\infty} \delta(p_i + k_i + sk - p_f - k_f)$$

- Mass shell condition for the propagator modified

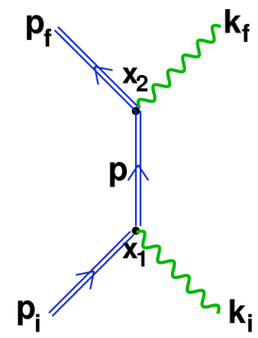

Consider ultrarelativistic electrons and headon laser...

$$\textit{No external field}: \quad \frac{1}{2(k_i p_i)} \approx \frac{1}{4\omega_i \epsilon_i} \qquad \textit{only IR divergence}$$

$$\textit{Bound State}: \quad \sum_{s=-\infty}^{\infty} \frac{1}{2(k_i p_i) - 2s(k p_i)} \approx \frac{1}{4\epsilon_i(\omega_i - s\omega)} \qquad \textit{additional divergences}$$

We must include radiative corrections
The potential SCS Resonances are observable!

Bound Interaction Picture I

- In bound state there is a 4-potential associated with an external source A^e, as well as the usual free Maxwell field,
- The coupling to the external field goes as $e|A^e|$. If the is strong enough then we must sum many terms

$$L_{IP} = -\tfrac{1}{4}F^{\mu\nu}F_{\mu\nu} + \bar{\psi}(i\gamma^\mu\partial_\mu - m)\psi + e\bar{\psi}(A + A^e)\psi$$

- "Dyson dilemma": nonzero radius of convergence in the perturbation series
- Solution: separate the external field part and put it in the Dirac part of the Lagrangian part

$$L_{BIP} = -\tfrac{1}{4}F^{\mu\nu}F_{\mu\nu} + \bar{\psi}(i\gamma^\mu\partial_\mu + eA^e - m)\psi + e\bar{\psi}A\psi$$

L_M L_{BD} L_I

The External classical potential

Bound Interaction Picture II

- Exact solution of the Bound Dirac equation for plane wave electromagnetic fields, [Volkov 1935, Bagrov, Gitman et al 1970s]

$$\left[1 + \frac{e}{2(k\cdot p)}\not{k}\not{A}^e\right]\exp\left(-i\int_0^{kx}\left[\frac{e(A^e\cdot p)}{(k\cdot p)} - \frac{e^2A^{e2}}{2(k\cdot p)}\right]d\phi\right)\exp(-ip\cdot x)\,u_s(p)$$

Spin dependent part including a magnetic moment interaction

An additional phase factor

The usual free fermion part

Bound Fermion Propagator
is 'dressed' by Volkov E functions

$$G^e(x-x') = E_p(x)G(x-x')\bar{E}_p(x)$$

where

$$\psi_V \equiv E_p(x)\exp(-ip.x)u_s(p)$$

New Feynman Rules
Only need a 'dressed' vertex

$$\gamma^e_\mu(p_f, p_i) = \bar{E}_{p_f}(x)\gamma_\mu E_{p_i}(x)$$

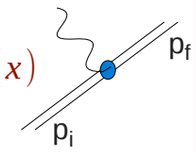

The SCS cross-section

- Transform the dressed vertices into momentum space – each contributing an infinite number of momentum modes

$$\sum_{s_1=-\infty}^{\infty}\sum_{s_2=-\infty}^{\infty}\delta^4\Big(p_f+\frac{e^2a^2}{2(k\cdot p_f)}k+k_f-p_i-\frac{e^2a^2}{2(k\cdot p_i)}k-k_i-(s_1+s_2)k\Big)$$

shifted momentum q_f, q_i shifted rest mass, $m+e^2a^2$

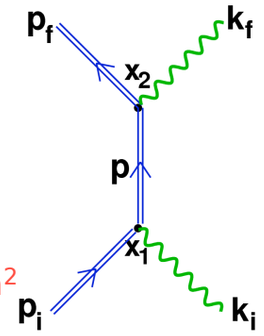

- Define an overall sum $s=s_1+s_2$, leaving one "internal summation" over s_1

$$M_{fi}=\sum_{s=-\infty}^{\infty}\left[\sum_{s_1=-\infty}^{\infty}\gamma^{e\mu}(p_f,p,s,s_1)\frac{1}{\not{q}_i-\not{k}_i+s_1\not{k}-m+i\epsilon}\gamma^{e\nu}(p,p_i,s,s_1)\right]$$

We can now derive the mass shell (resonance) conditions

SCS resonance conditions

- Direct Channel

$$s_1=\frac{(q_i\cdot k_i)}{(k\cdot p_i)+(k\cdot k_i)}=\frac{\omega_i}{\omega}\frac{1+\frac{e^2a^2}{2}(1+\cos\theta_i)}{1+\omega_i(1-\cos\theta_i)}$$

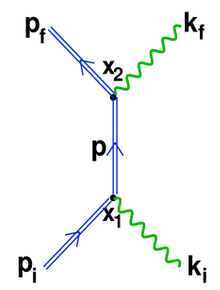

- Exchange channel

$$s_1=-\frac{(q_f\cdot k_i)}{(k\cdot p_i)-(k\cdot k_f)}=-\frac{\omega_f}{\omega}\frac{1+\frac{e^2a^2}{2}(1-\cos\theta_f)}{1-\omega_f(1-\cos\theta_f)}$$

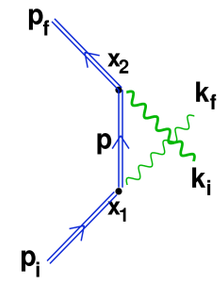

- Resonance width (energy level width $\Delta\varepsilon_p$)

$$\cos\Delta\theta_i\approx\left|1-\frac{2\epsilon_p\Im\Delta\epsilon_p}{\omega_i(e^2a^2/2+s_1\omega)+\omega_i+s_1\omega}\right|$$

Now we need to calculate the self energy in an external field

The bound state resonance width

In analogy to normal QED, the geometric sum of self energy loop corrections leads to a mass shift (real and imaginary) in the propagator denominator

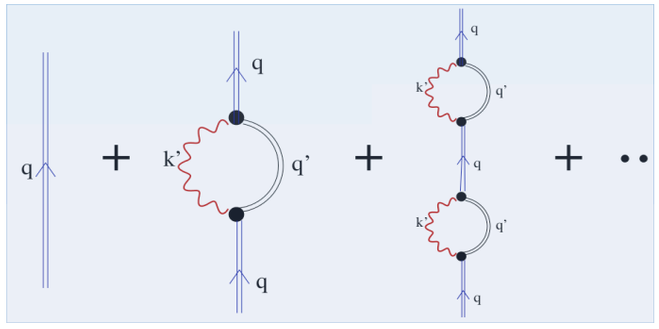

$$G_q^e+G_q^e\Sigma_q^eG_q^e+G_q^e\Sigma_q^eG_q^e\Sigma_q^eG_q^e+\cdots=\int\frac{d^4q}{(2\pi)^4}E_q\frac{1}{\not{q}-m+\Sigma_q^e+i\epsilon}\overline{E}_q$$

Provides a damping factor

$\approx Ai(\epsilon_q)$ constant crossed field

$\approx J_0(\epsilon_q)$ circularly polarised field

Regularization/Renormalization
"only necessary for the interaction with the vacuum"
(Ritus 1971)

I find no UV divergence!

Additional radiative corrections

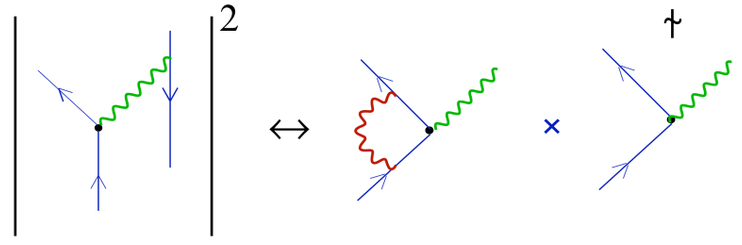

'normal' QED
Vertex correction same order as Bremstrahlung process

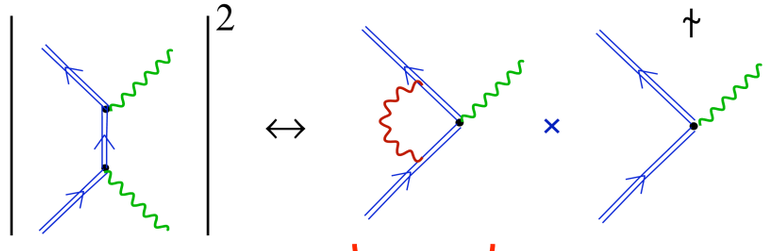

strong field QED
Vertex correction same order as our SCS process

We need to calculate Γ^{ev} using exact solutions in the external field

Is there a strong field QED Ward identity?

$$\frac{\partial}{\partial f(q)}\Sigma^e(q)\Leftrightarrow\Gamma^{e\mu}$$

Numerical Simulation/Experiment

Required: A high intensity laser, a probe laser on moveable stage, a photon detector and an electron beam

High intensity laser: Table Terawatt lasers (Sprangle 1992)
(a) 5 eV photons with irradiance 2×10^{19} W/cm^2
(b) 1200 keV photons with irradiance 1.5×10^{17} W/cm^2

- Laser photon (k) energy ω in natural units

$$\frac{\hbar\omega}{mc^2} = \text{(a) } 10^{-5}, \text{(b) } 2.4$$

- laser field intensity parameter

$$\nu = \frac{eE}{\omega mc} \approx 1$$

- Incident laser (k_i) angle θ_i
- Scattered photon (k_f) angles θ_f, ϕ_f

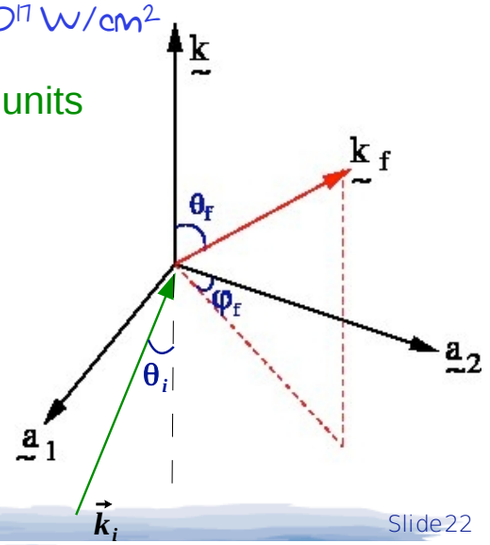

Stimulated Compton Scattering x-section

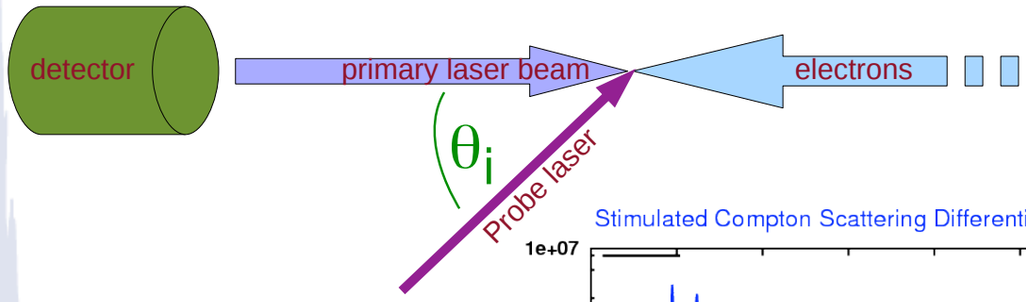

Primary laser: 25.6 keV photons, $\nu^2=1$
Probe laser: 51.2 keV, variable incident angle

scattered photon resonances at $\theta_i \approx \pm 60^o$

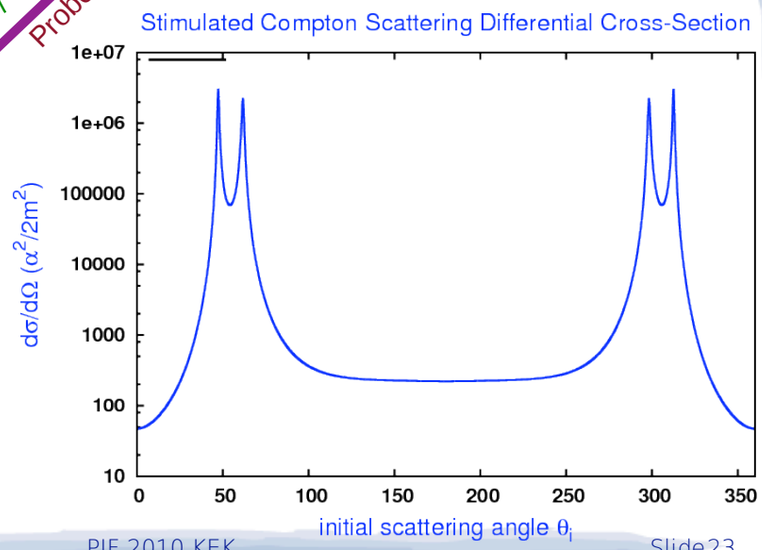

Stimulated Compton Scattering x-section

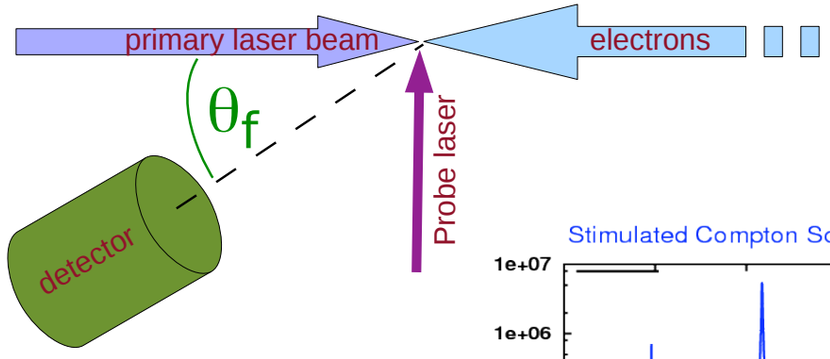

Primary laser: 61 keV photons, $\nu^2=0.1$
Probe laser: 51.2 keV, 90^o incident angle

Multiple scattered photon resonances

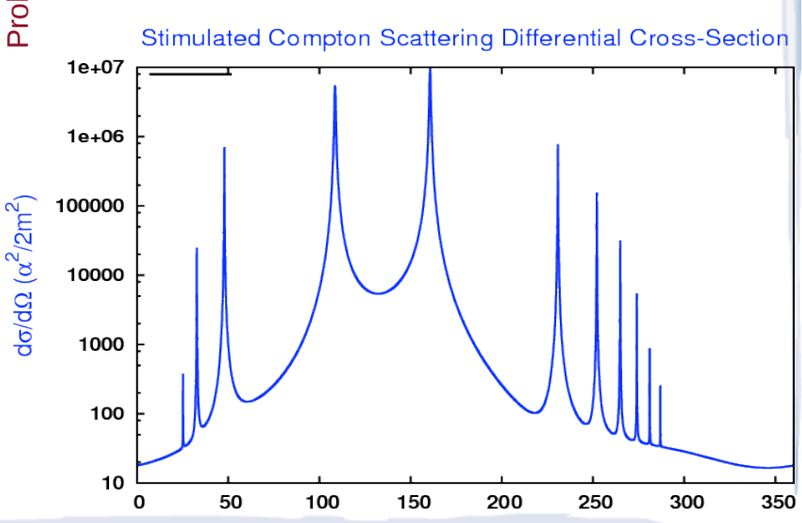

Summary/Future motivation

- The study of strong field physics is theoretically challenging and very interesting
- Using exact solutions of the Dirac equation in the presence of the 'strong' field, Nonlinear cross-sections can be calculated analytically

- The second order processes are particularly interesting because of the behaviour of their propagators.
- Theoretical Radiative corrections in the strong field are still being calculated – Vertex Correction

- The application of the strong field radiative corrections is essential to produce realistic numerical simulations
- The availability of intense laser/electron beam interactions mean that these effects can and should be studied experimentally

“Radiation damping” experiment at ATF2

door to the regimes of dominant radiation reaction

1.3GeV

1.2GeV

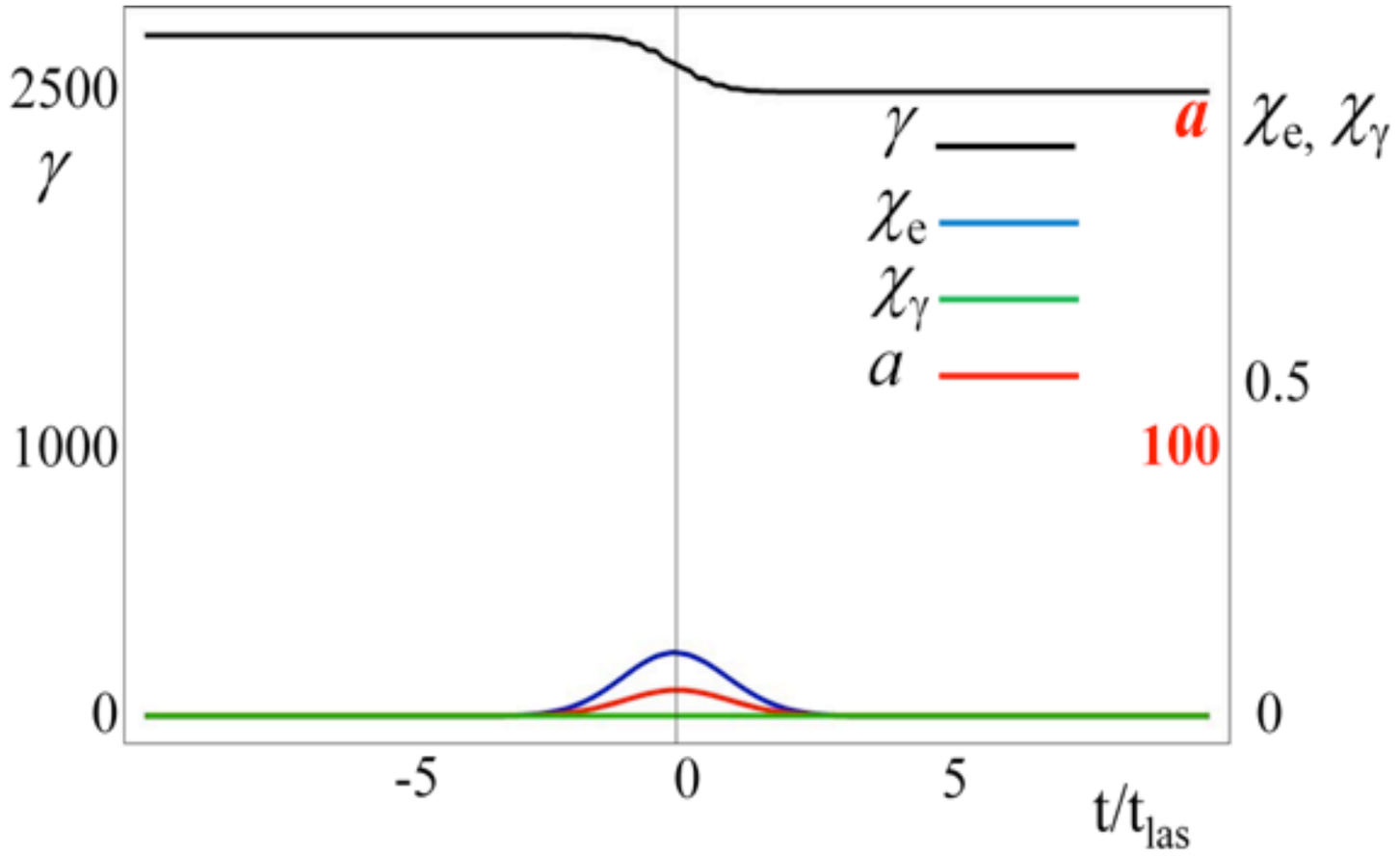

Time dependence of the electron and photon parameters for a 1.3 GeV electron beam interacting with a 30 fs laser pulse (a0=9.9): the electron energy - black; parameter e - blue; laser pulse profile – red, parameter γ - green.

Ref : ON THE DESIGN OF EXPERIMENTS FOR THE STUDY OF EXTREME FIELD LIMITS IN THE INTERACTION OF LASER WITH ULTRA RELATIVISTIC ELECTRON BEAM, S.V.Bulanov et al., eprint arXiv:1101.2501

S.V.Bulanov et al., eprint arXiv:1101.2501

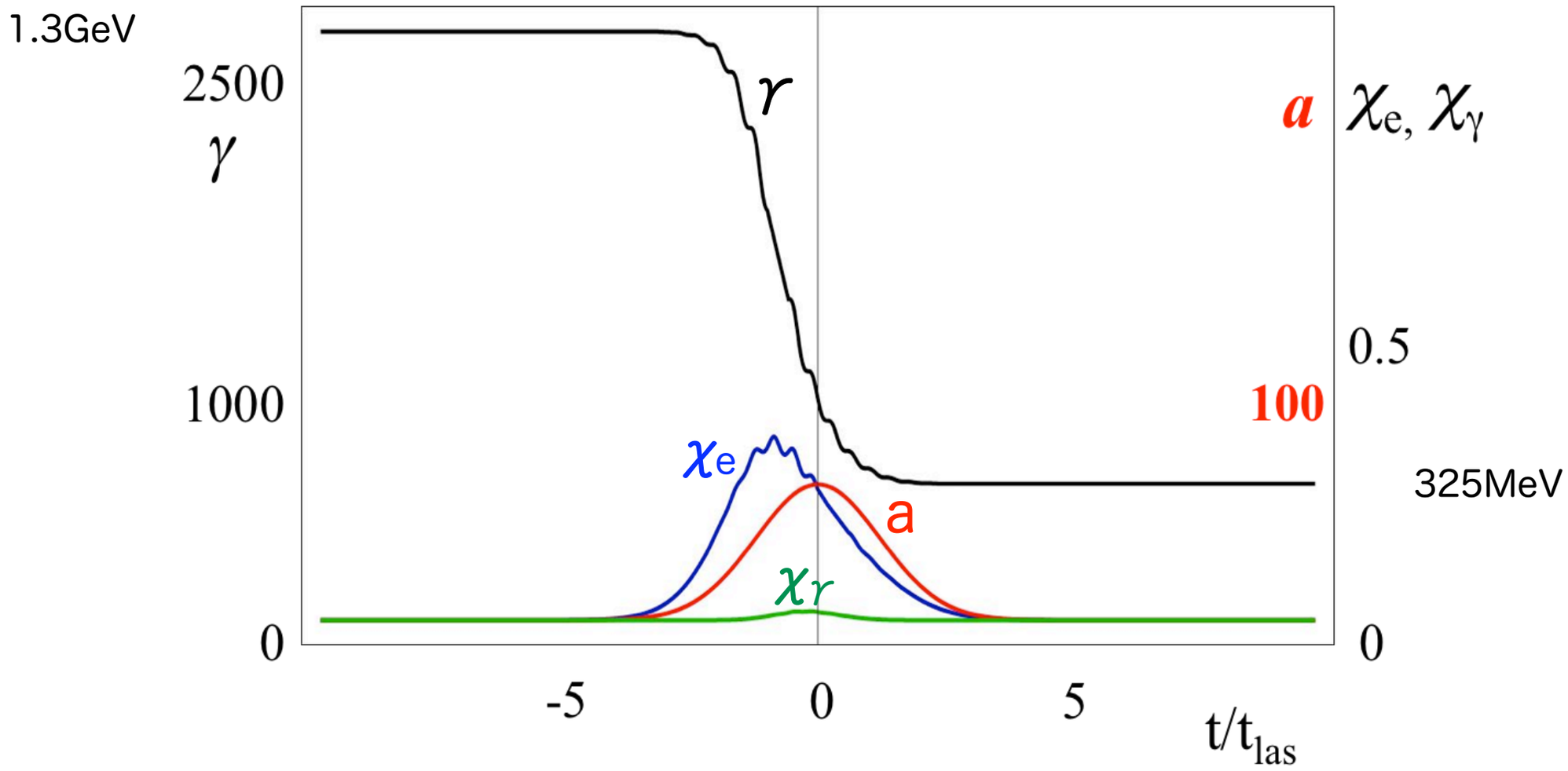

Time dependence of the electron and photon parameters for a 1.3 GeV electron beam interacting with a 30 fs laser pulse (a0=60): the electron energy - black; parameter - blue; laser pulse profile – red, parameter - green. by S. Bulazov, Dec 2010

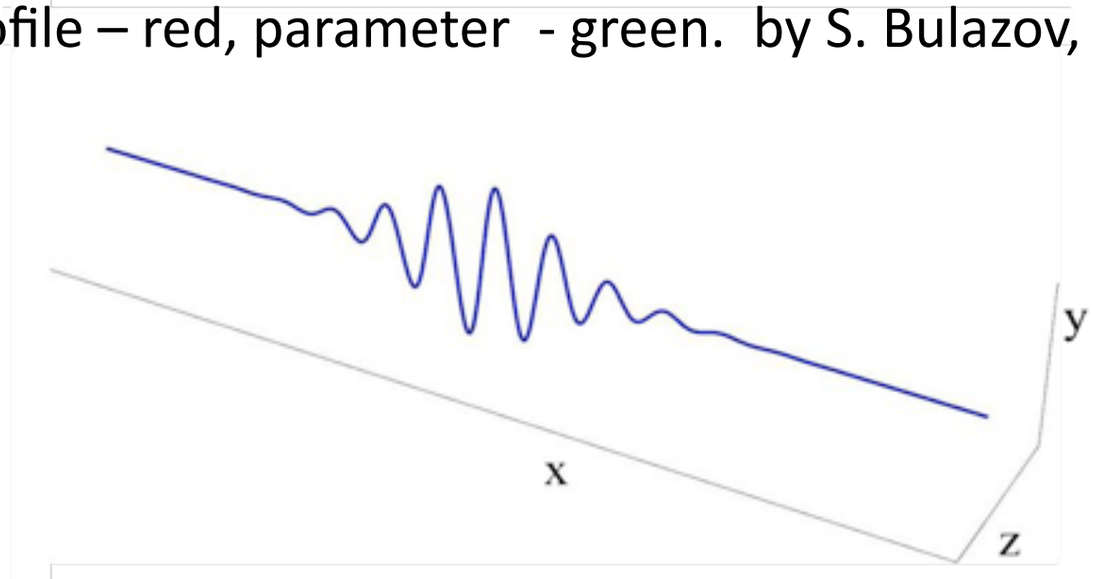

electron trajectory for a_0=60

S.V.Bulanov et al., eprint arXiv:1101.2501

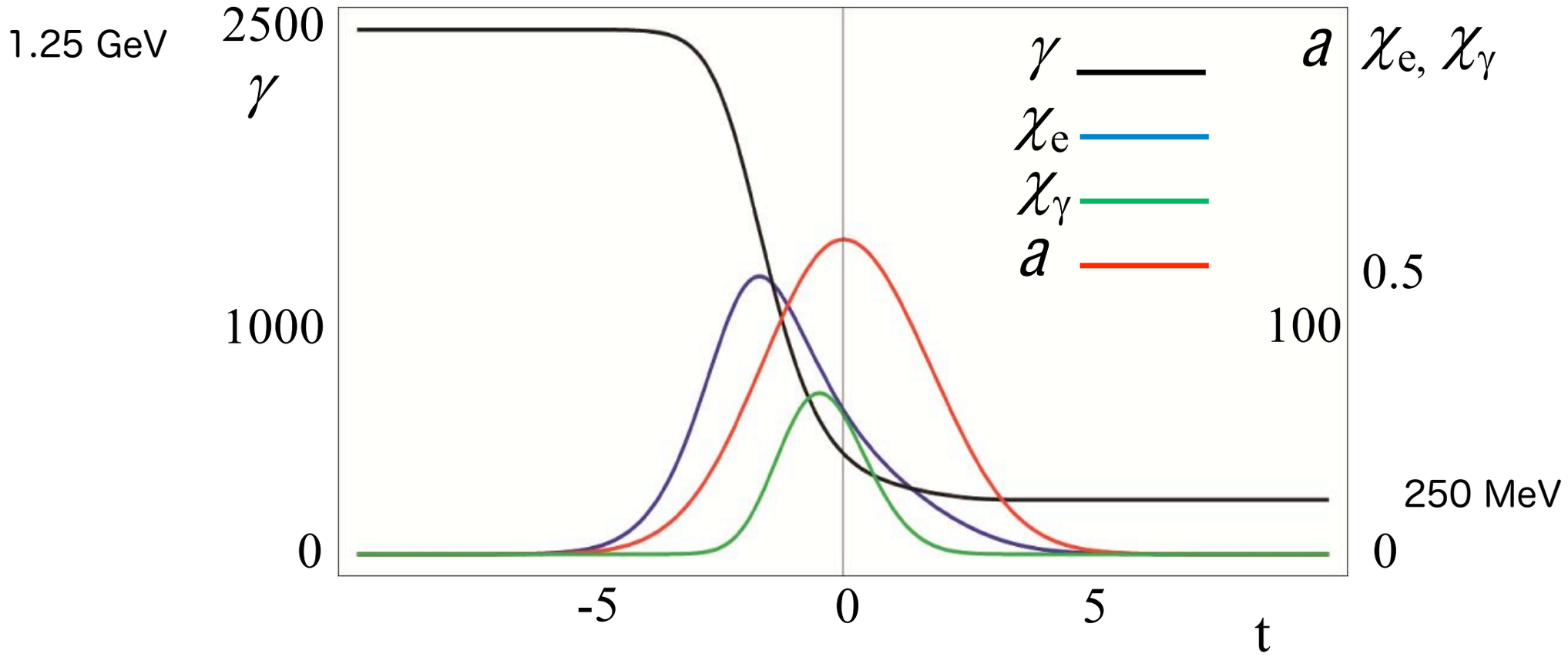

Figure 5. Time dependence of the electron and photon parameters for a 1.25 GeV electron beam interacting with a 15 fs PW laser pulse ($a_0 = 100$): the electron energy - black; parameter χ_e - blue; laser pulse profile – red, parameter χ_γ - green.

Note : e+e- pairs will be created for χ_γ =0.3 in collisions between 1.25GeV electron and laser with a_0=100.

Study of visibility of Compton recoil electrons in the presence of halo after the IP of ATF2

By C. CHAO

July 2011

Without quad

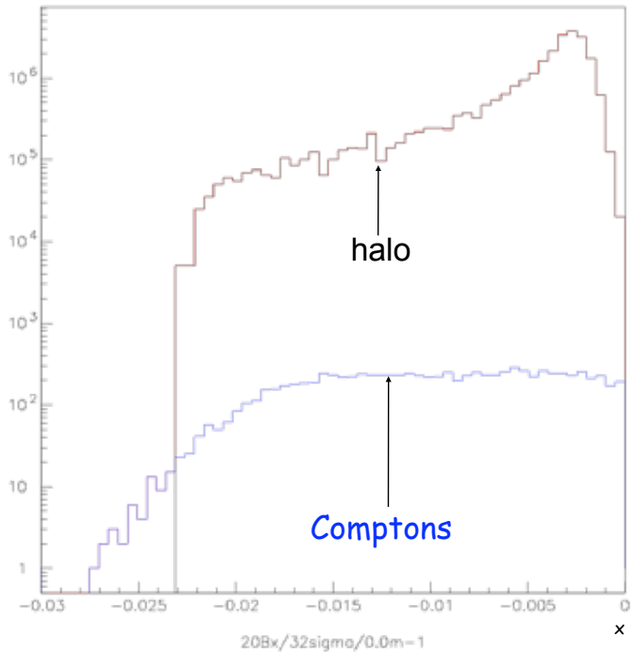

X distribution

Comptons are difficult to detect without quad (unless tighter collimation is used)

- Shape of x' and y' distribution▪:
  $2.2 \times 10^9 \times x^{-3.5}$ from 3σ to 6σ
  $3.7 \times 10^8 \times x^{-2.5}$ outside 6σ

Illustrative layout

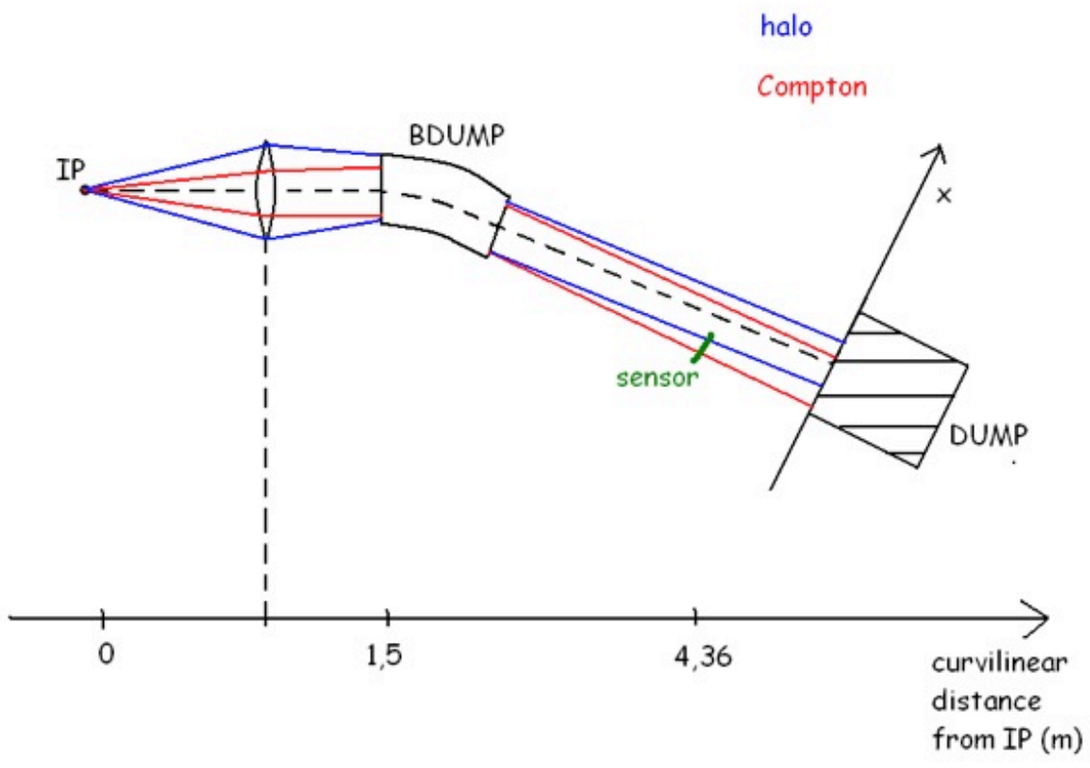

With quad (QM7R)

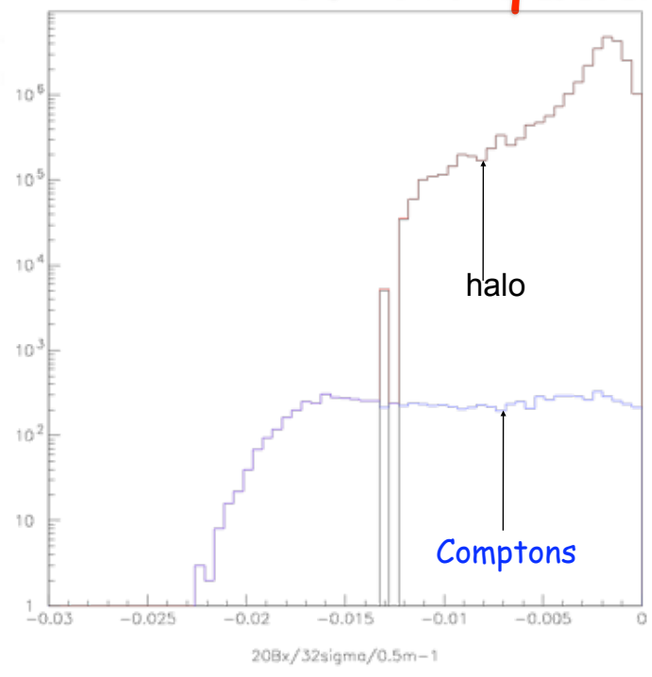

X distribution

For quad strength of $0{,}5m^{-1}$, we could detect Comptons

Black Hole Evaporation ?

Credit: Jörn Wilms (Tübingen) et al.; ESA

Hawking Radiation in Black Hole

(1) Photon production

in vacuum near the horizon

(2) The energy spectrum

in the Planck distribution

"Vacuum polarization near Event Horizon"
, but Thermal radiation

The same phenomenon would be realized in an accelerated system by Principle of Equivalence between gravitational and inertial forces .

Unruh Radiation in Acceleration

expect the interaction of electrons in ultra-intense fields,

i.e. electron beams and the lasers

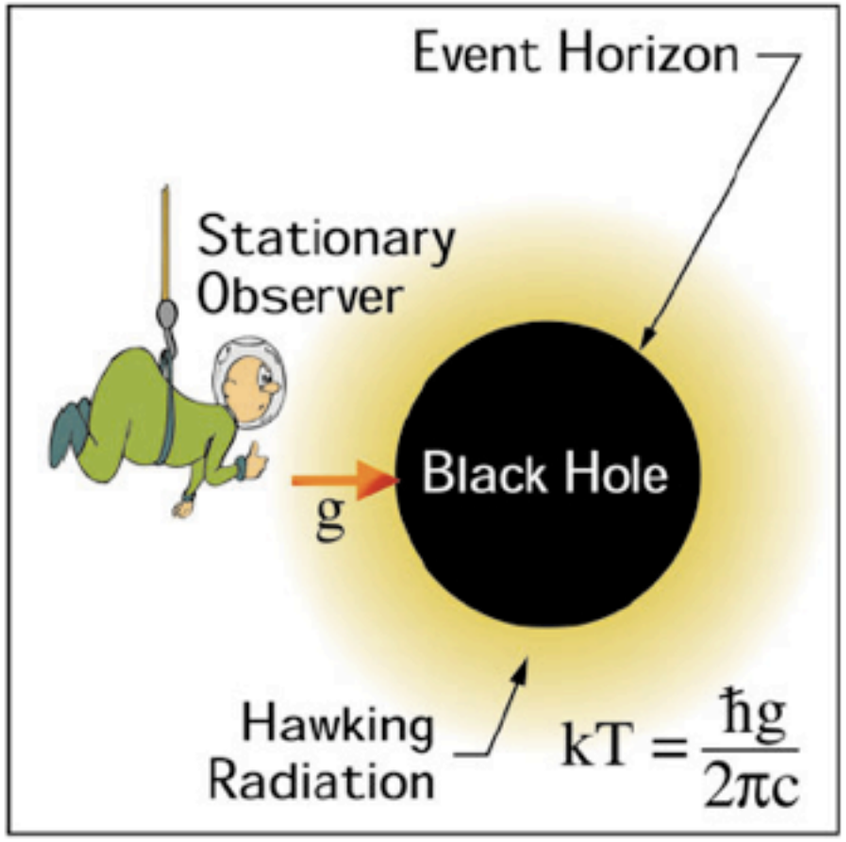

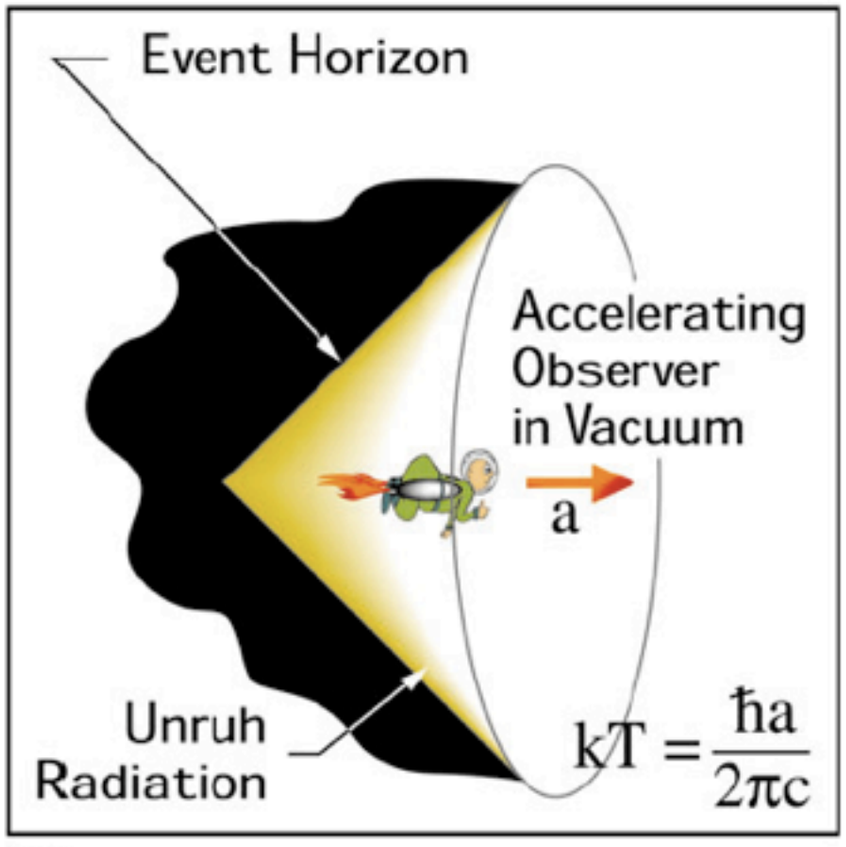

Fig. 11: Analogy between Hawking and Unruh effects.
Pisin Chen, AAPPS Bulletin February 2003

Signatures of the Unruh effect in strong lasers?

Ralf Schützhold

Fachbereich Physik

Universität Duisburg-Essen

UNIVERSITÄT DUISBURG ESSEN

Differences

- angular dependence (blind spot)
- photon statistics
  Unruh: squeezed state (pairs)
  Larmor: coherent state (Poisson)
- polarization
  → vacuum entanglement
- spectral dependence ($k < k_{\rm cut}$)
  Unruh: $1/k^2$ vs Larmor: $1/k^3$
- detectable in future facilities?
  Schwinger: $E_S = \mathcal{O}(10^{18}\,{\rm V/m})$
- Schwinger effect, back-reaction?

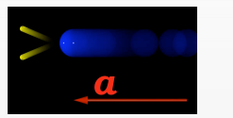

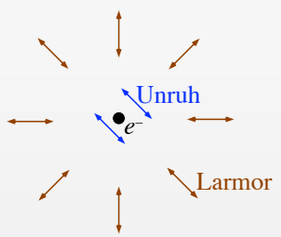

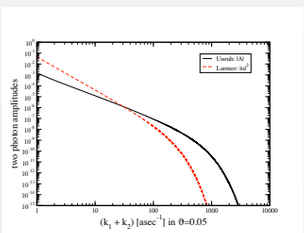

R. S., G. Schaller, and D. Habs, Phys. Rev. Lett. **97**, 121302 (2006).

Constant Electric Field ($\dot{a} = 0$)

R. S., G. Schaller, and D. Habs, Phys. Rev. Lett. **97**, 121302 (2006).

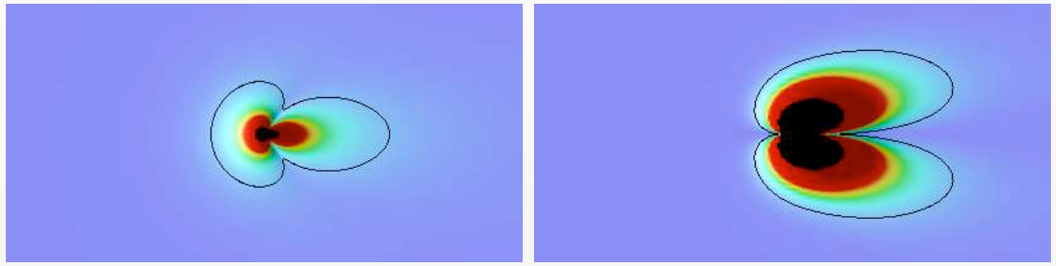

Unruh radiation Larmor radiation

→ blind spot: quantum (Unruh) radiation dominates within small forward cone with angle

$$\vartheta = \mathcal{O}\left(\frac{1}{\gamma}\sqrt{\frac{E}{E_S}}\right)\ ,\ \mathfrak{P}_{\rm Unruh}(\vartheta) = \mathcal{O}\left(\frac{E^4}{E_S^4}\right) \ll 1$$

Schwinger limit $E_S = m_e^2/q_e = \mathcal{O}(10^{18}\,{\rm V/m})$

Alternative Set-up

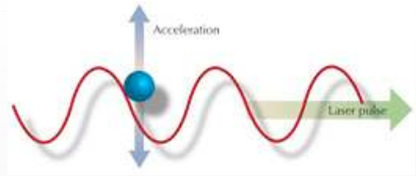

http://www.extreme-light-infrastructure.eu/

Lowest-order Feynman diagrams

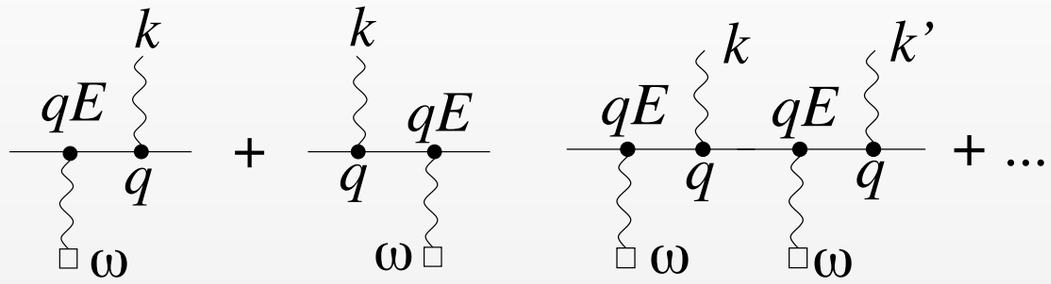

→ $\omega = k$ → classical (Larmor, Thomson) radiation

However, further diagrams, e.g.: yield $\omega = k + k'$ and can not be explained within classical electrodynamics…

→ **Unruh effect**

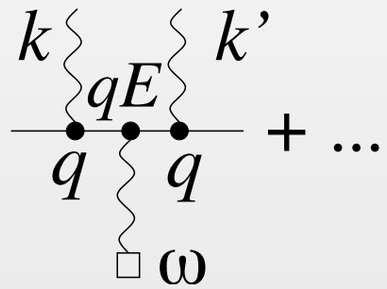

Lowest-order Scaling

Quantum (Unruh) radiation (cf. E^4/E_S^4)

$$\mathfrak{P}_{\text{Unruh}} = \frac{\alpha_{\text{QED}}^2}{4\pi}\left[\frac{E}{E_S}\right]^2 \times \mathcal{O}\left(\frac{\omega T}{30}\right)$$

Classical (Larmor) counterpart (i.e., background)

$$\mathfrak{P}^{1\gamma}_{\text{Larmor}} = \alpha_{\text{QED}}\left[\frac{qE}{m\omega}\right]^2 \times \mathcal{O}\left(\frac{\omega T}{2}\right)$$

One electron with $\gamma = 300$ after 100 cycles
in Laser field with 10^{18}W/cm^2 yields
$\mathfrak{P}_{\text{Unruh}} = 4 \times 10^{-11}$ and $\mathfrak{P}^{1\gamma}_{\text{Larmor}} = \mathcal{O}(10^{-1})$
e.g., $N_e = 6 \times 10^9$ ...

Distinguishability

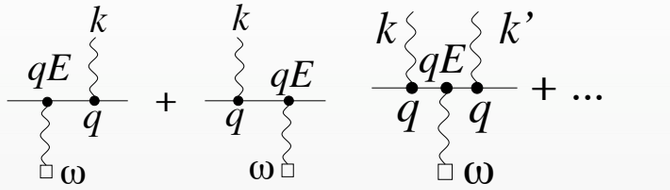

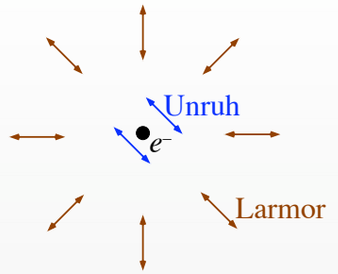

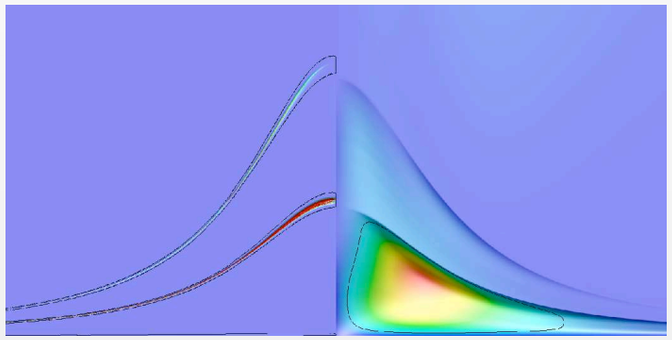

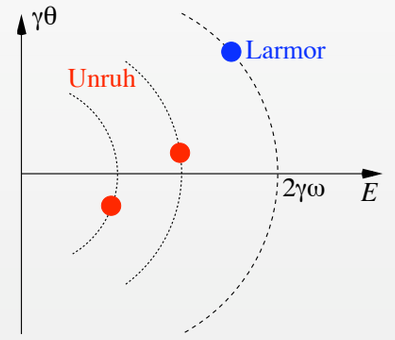

Larmor (classical) $\leftrightarrow$ Unruh (quantum)

$\rightarrow$ energy, polarization, coincidence

R. S., G. Schaller, and D. Habs, Phys. Rev. Lett. **100**, 091301 (2008).

Beyond Perturbation Theory...

Coherent state (Larmor radiation)

$$|\alpha\rangle = \exp\{\alpha\hat{a}^\dagger - \alpha^*\hat{a}\}|0\rangle \rightsquigarrow \langle\alpha|\,\hat{n}\,|\alpha\rangle = |\alpha|^2 \propto N_e^2$$

Squeezed state (Unruh signatures)

$$|\xi\rangle = \exp\left\{\frac{\xi}{2}\hat{a}^2 - \text{h.c.}\right\}|0\rangle \rightsquigarrow \langle\xi|\,\hat{n}\,|\xi\rangle = \sinh^2(|\xi|)$$

$\rightarrow$ exponential growth above threshold

$$N_e^{\text{bunch}} = \mathcal{O}\left(\frac{E_S}{\alpha_{\text{QED}}E}\right)$$

Photon-pair laser?!?

Summary

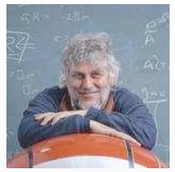

- signatures of Unruh effect detectable in near-future facilities?!?

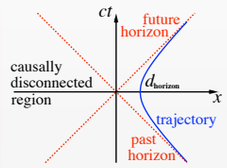

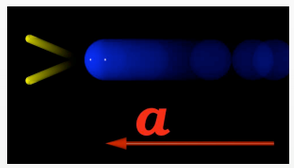

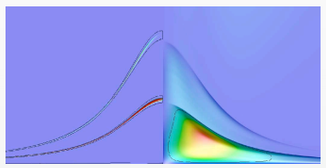

- vacuum entanglement $\rightarrow$ entangled pairs
  polarization, energy, and possibly momentum
- source for entangled photon pairs
  quantum-optics applications in the keV regime
- relation to Hawking and Schwinger effect
  $\rightarrow$ talk by G. Dunne

R. S., G. Schaller, and D. Habs, Phys. Rev. Lett. **97**, 121302 (2006);
Phys. Rev. Lett. **100**, 091301 (2008).

European proposal titled “Studying the Unruh effect using high-power, short-pulse lasers

Experimental Scenarios

Table 1. Correlation between laser intensity, electric field, electron acceleration, resulting Unruh temperatures and event horizon distances.

vacuum temperature

method	I [W/cm^2]	E [V/m]	$\hbar\omega$ [eV]	a [g]	kT_{Unruh} [keV]	horizon distance d
laser focus	10^{23}	10^{15}	1	$2\cdot 10^{25}$	$8\cdot 10^{-2}$	0.5 nm
+ coherent harmonic focussing	$5\cdot 10^{29}$	$1.3\cdot 10^{18}$	1	$2\cdot 10^{28}$	80	0.5 pm
+ Lorentz boost ($\gamma = 10^3$)	$2\cdot 10^{36}$	$3\cdot 10^{21}$	1	$4\cdot 10^{31}$	$1.6\cdot 10^{5}$	0.3 fm

Schwinger field

quark-gluon plasma transition

Extra dimensions distance scale

DFG Cluster of Excellence MAP (Munich-Centre for Advanced Photonics)

"Tabletop Creation of Entangled Multi-keV Photon Pairs and the Unruh Effect", Ralf Schu¨tzhold et al., PRL 100, 091301 (2008)

Method-1

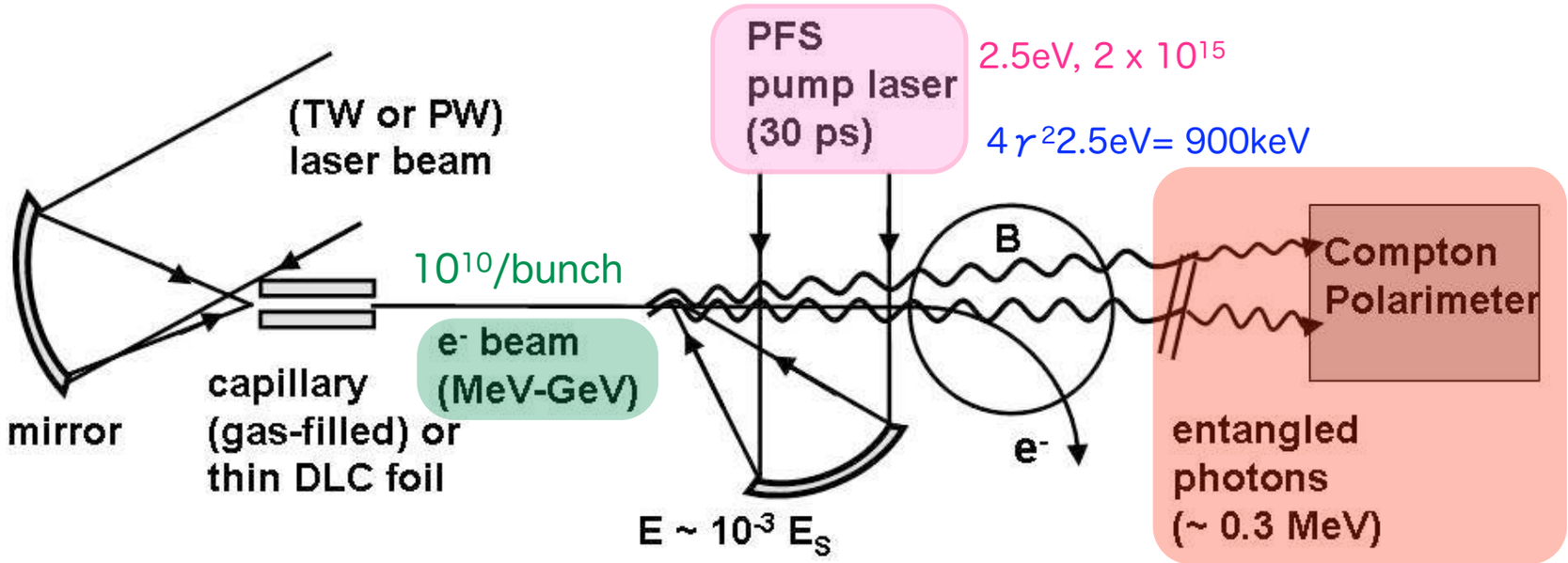

Fig. 5. Schematical view of an experimental setup for the detection of Unruh radiation originating from laser-accelerated energetic electrons interacting with the strong periodic field of a counter-propagating optical laser beam.

Method-2

preferable for less Larmor and larger Unruh radiation

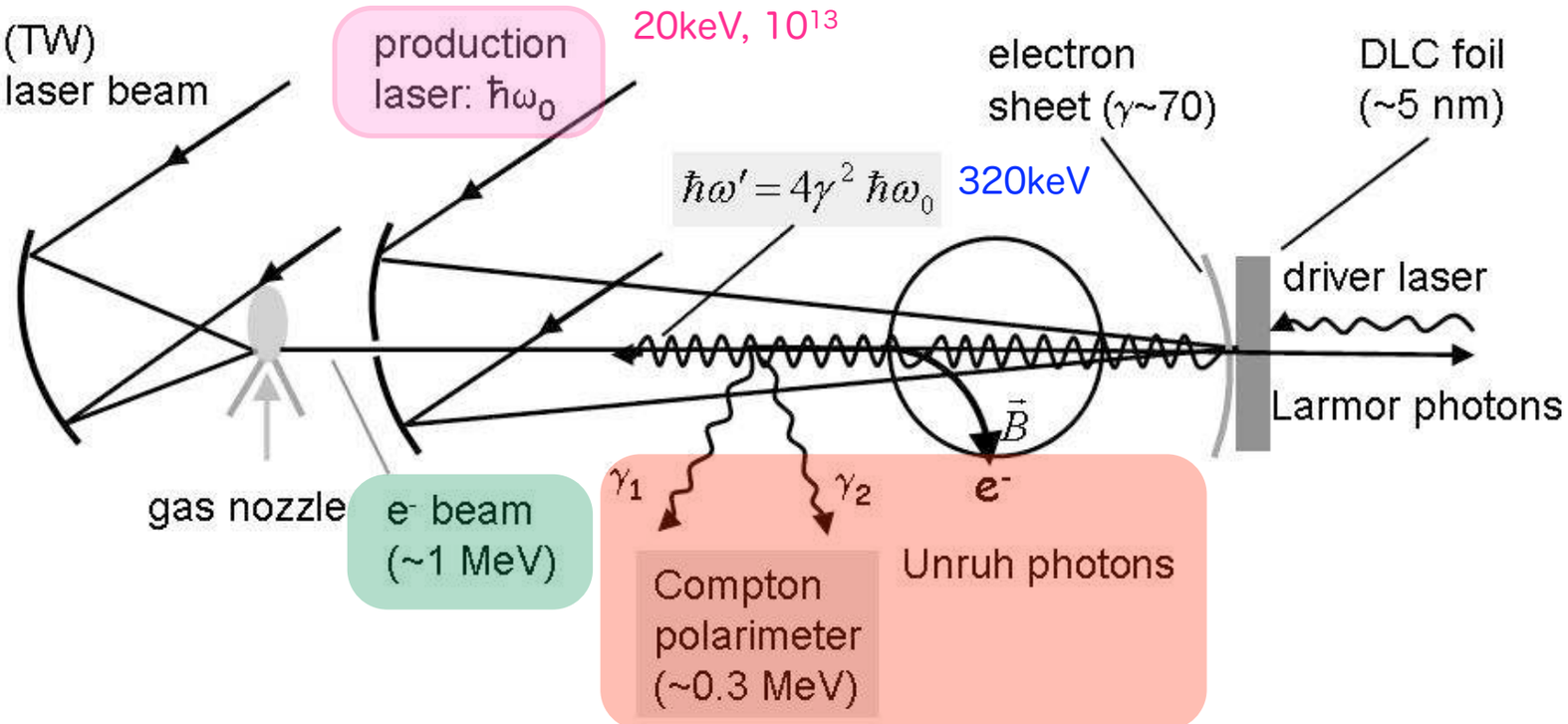

Fig. 6. Schematical view of an experimental setup for the detection of Unruh radiation originating from laser-accelerated low-energy electrons interacting with a brilliant X-ray beam produced from reflecting an optical laser beam off a relativistic dense electron sheet (see text) used as undulator.

Table 2. Comparison of relevant parameters given for the two experimental scenarios discussed in the text for the creation of Unruh photon pairs with a summed energy of 900 keV (320 keV) for the scenario listed in the top (bottom) row.

Method	N_γ /bunch	$E_{kin,e}$ [MeV]	γ	I^{lab} [W/cm^2]	I^{int} $(2\gamma)^2$ [W/cm^2]	$\hbar\omega_0$ (*:$\hbar\omega'$) [eV]	$\hbar\omega_{int}$ 2γ [eV]	E^{lab} [V/m]	E^{int} 2γ [V/m]	a [g]	kT_U 2γ [eV]	hor. dist. d [m]	a_0
1	$2\cdot 10^{15}$	150	300	10^{18}	$3.6\cdot 10^{23}$	2.5	$1.5\cdot 10^{3}$	$1.9\cdot 10^{12}$	$1.2\cdot 10^{15}$	$2.1\cdot 10^{25}$	80	$4\cdot 10^{-10}$	0.3
2	10^{13}	1	2	$2\cdot 10^{25}$	$3.2\cdot 10^{26}$	$2\cdot 10^{4}$ *	$8\cdot 10^{4}$	$8.7\cdot 10^{15}$	$3.5\cdot 10^{16}$	$6.2\cdot 10^{26}$	$2.2\cdot 10^{3}$	$1.5\cdot 10^{-11}$	0.2

1. Experiment for Unruh radiation

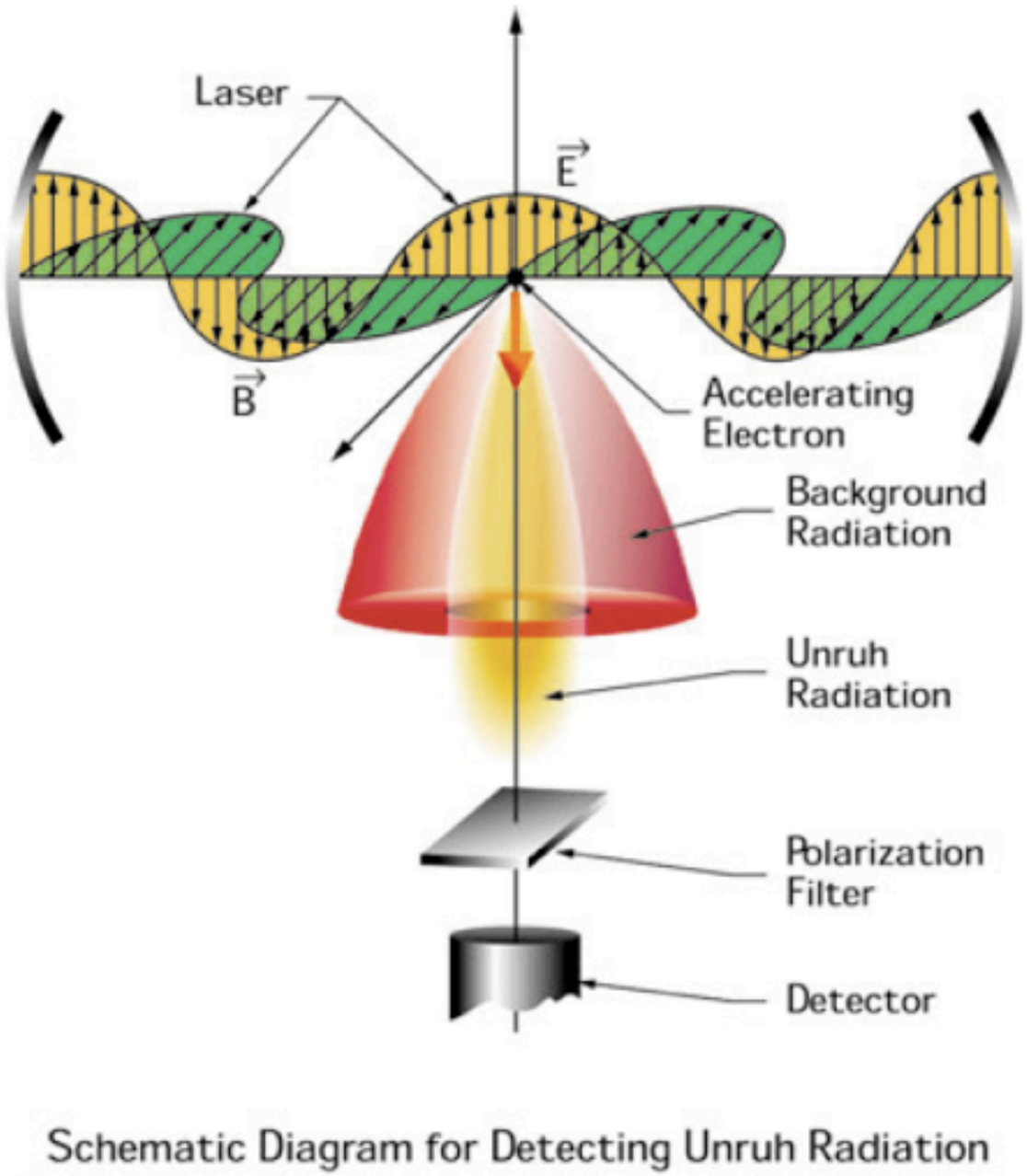

Schematic Diagram for Detecting Unruh Radiation

5-2000
8544A2

Fig. 12: A conceptual design of an experiment for detecting the Unruh effect.

Facilities at KEK

Nanometer electron beam at ATF2

1.3GeV energy

37nm vertical beam size at IP

Ultra-intense Laser beam in future

λ = 0.8 um

intensity >10^{20}W/cm^2

Unruh radiation ∝ a_o^3

Acceleration ($a_o \omega c$)=3.4x10^{25}m/s^2

Photon Energy vs. Angle

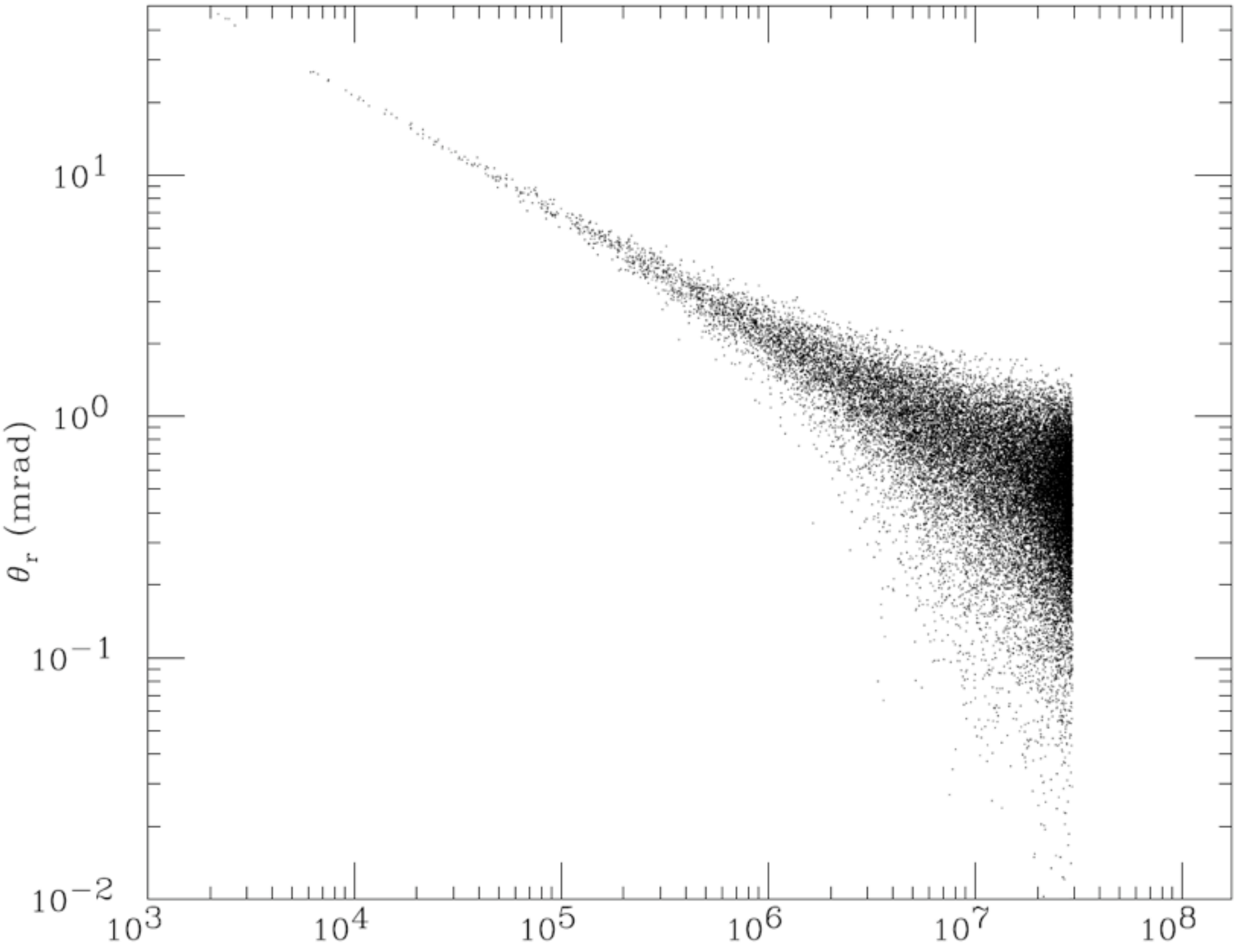

Photon (x,y) Angle, E<100keV

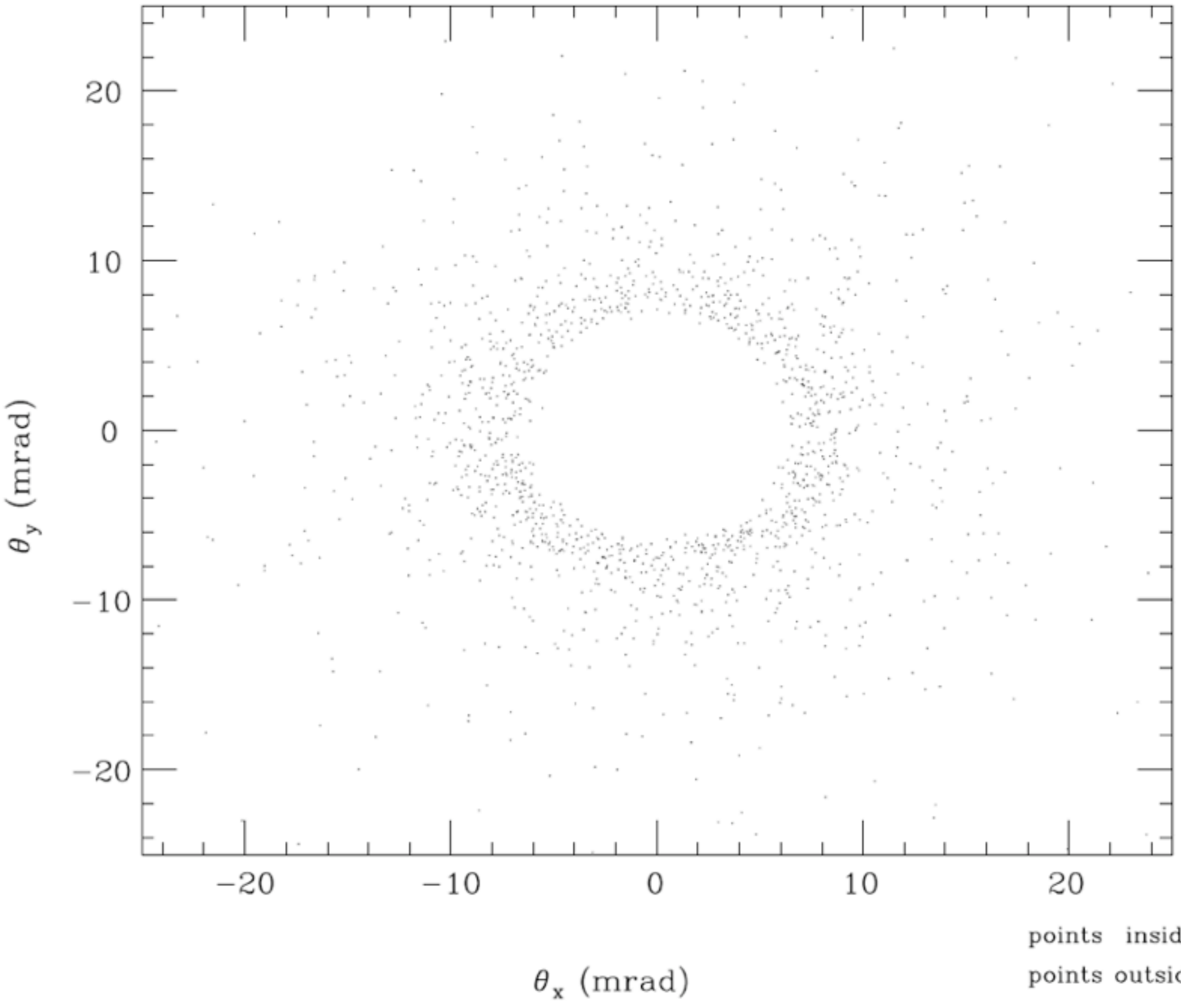

points inside 1561
points outside 101

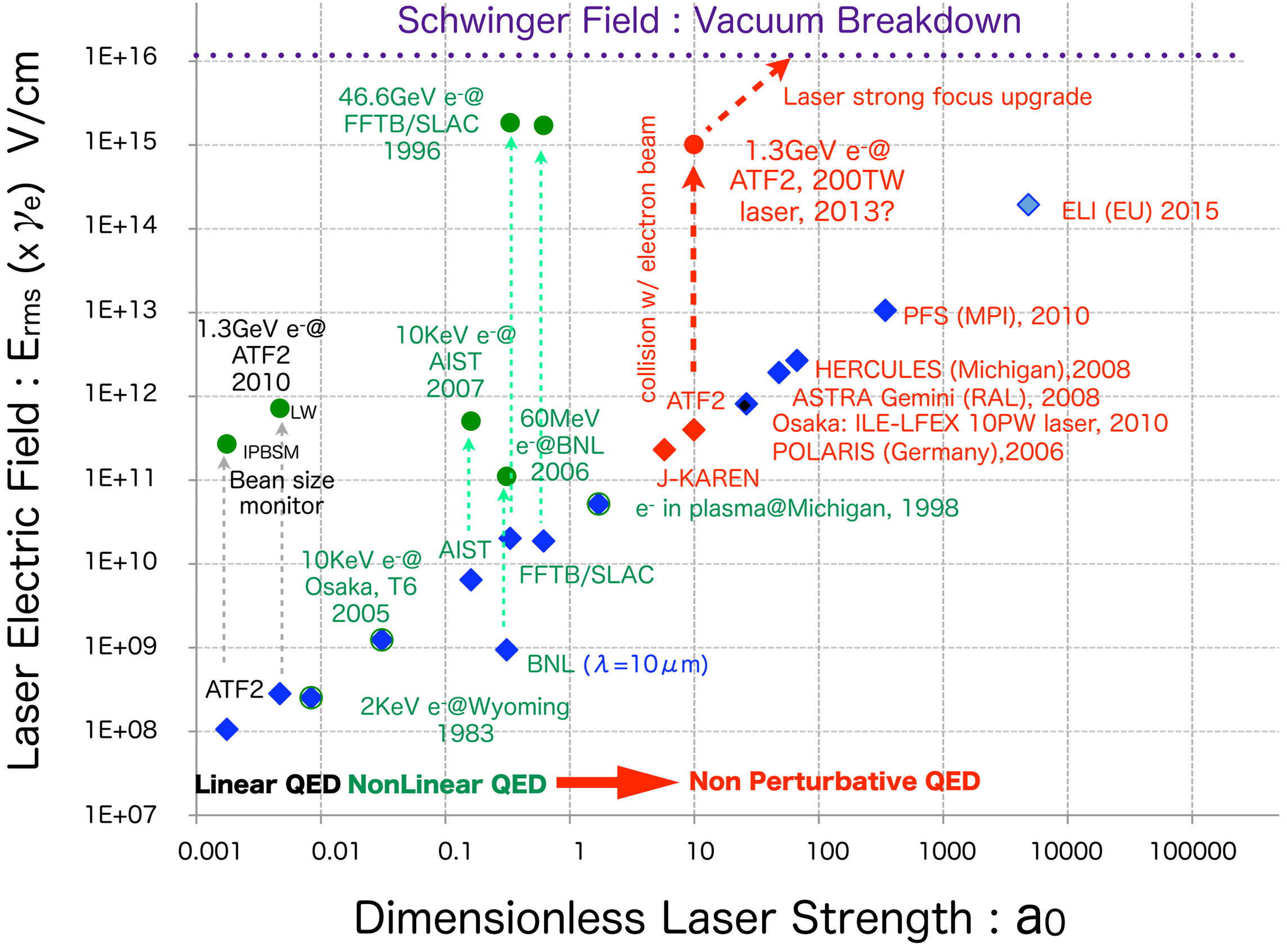
Schwinger Field : Vacuum Breakdown
Laser Electric Field : Erms (x γe) V/cm
1E+16
1E+15
1E+14
1E+13
1E+12
1E+11
1E+10
1E+09
1E+08
1E+07
0.001
0.01
0.1
1
10
100
1000
10000
100000
Dimensionless Laser Strength : a0
46.6GeV e-@ FFTB/SLAC 1996
Laser strong focus upgrade
1.3GeV e-@ ATF2, 200TW laser, 2013?
collision w/ electron beam
ELI (EU) 2015
PFS (MPI), 2010
HERCULES (Michigan),2008
ASTRA Gemini (RAL), 2008
Osaka: ILE-LFEX 10PW laser, 2010
POLARIS (Germany),2006
ATF2
J-KAREN
1.3GeV e-@ ATF2 2010
LW
IPBSM
Bean size monitor
10KeV e-@ AIST 2007
60MeV e-@BNL 2006
e- in plasma@Michigan, 1998
AIST
FFTB/SLAC
10KeV e-@ Osaka, T6 2005
BNL (λ=10μm)
ATF2
2KeV e-@Wyoming 1983
Linear QED
NonLinear QED
Non Perturbative QED

Summary of Prospect at ATF2 with 200TW laser

1. Strong QED : Non-linear Compton scattering, and radiation damping etc.
   Experiments in unexplored region, a_0 =10~60

2. Unruh radiation, i.e. physics at the event horizon

3. Plasma focussing
   - measurement of beam size by Shintake monitor

4. Plasma acceleration (2.1TeV of energy gain in $n=10^{18}/cm^3$)
   - 10GeV/cm means 1TeV/m !
   - demonstration with energy spectrometer